NeuroImage **10,** 233–260 (1999)
Article ID nimg.1999.0459, available online at http://www.idealibrary.com on IDEAL®

Three-Dimensional MRI Atlas of the Human Cerebellum in Proportional Stereotaxic Space

Jeremy D. Schmahmann,* Julien Doyon,†‡ David McDonald,‡ Colin Holmes,§ Karyne Lavoie,†
Amy S. Hurwitz,* Noor Kabani,‡ Arthur Toga,§ Alan Evans,‡ Michael Petrides‡¶

**Department of Neurology, Massachusetts General Hospital and Harvard Medical School, Boston, Massachusetts; †Department of Psychology, and Rehabilitation Research Group, Francois-Charon Center, Laval University, Quebec City, Canada; ‡McConnell Brain Imaging Center, and ¶Cognitive Neuroscience Unit, Montreal Neurological Institute, and McGill University, Montreal, Canada; and §Laboratory of Neuroimaging, Department of Neurology, University of California School of Medicine, Los Angeles, California*

Received February 11, 1999

We have prepared an atlas of the human cerebellum using high-resolution magnetic resonance-derived images warped into the proportional stereotaxic space of Talairach and Tournoux. Software that permits simultaneous visualization of the three cardinal planes facilitated the identification of the cerebellar fissures and lobules. A revised version of the Larsell nomenclature facilitated a simple description of the cerebellum. This atlas derived from a single individual was instrumental in addressing longstanding debates about the gross morphologic organization of the cerebellum. It may serve as the template for more precise identification of cerebellar topography in functional imaging studies in normals, for investigating clinical–pathologic correlations in patients, and for the development of future probabilistic maps of the human cerebellum.

Key Words: **cerebellum; atlas; anatomy; human; proportional stereotaxic (Talairach) space; brain mapping.**

As clinical and functional magnetic resonance imaging (MRI) technology continues to improve, the ability to differentiate cerebellar lobules and folia on all planes of section has become quite precise. There is a problem, however, in correlating this technology with the knowledge of cerebellar anatomy because there is no atlas that can be reliably used for the accurate identification of the different cerebellar regions. Terms such as medial/lateral, anterior/posterior, or vermis/hemisphere are generally used in clinical studies, but these terms are anatomically vague. In functional imaging studies using positron emission tomography (PET) and functional magnetic resonance imaging (fMRI) when the locations of cerebellar activations are presented as Talairach coordinates, it has generally not been possible to identify precisely which cerebellar lobule or folium is involved. The atlas of Talairach and Tournoux (1988) itself has no anatomic structures depicted within the sketched outlines of the cerebellum.

Available cerebellar atlases depict major landmarks but they are generally limited to gross morphologic relationships and they cannot localize brain structures activated in PET and fMRI studies (e.g., Crosby *et al.*, 1962; Carpenter, 1976; DeArmond *et al.*, 1976; Waddington, 1984; Roberts *et al.*, 1987; Kretshmann and Weinrich, 1992). In these atlases the individual cerebellar lobules are generally not labeled, and only limited sections are available in either one or two of the cardinal planes. More recent attempts to address these concerns using MRI (Courchesne *et al.*, 1989; Press *et al.*, 1989, 1990) are useful, but they are limited by the relatively small number of sections presented and the spatial resolution.

The most detailed available atlas of the human cerebellum is that of Angevine *et al.* (1961). This dissection in three planes reveals the structure of the folia and deep nuclei. There are inherent difficulties in using this atlas for contemporary purposes, however. It is applicable only in the parasagittal plane, as the coronal and axial planes of sections shown are dissimilar from those used in clinical and functional neuroimaging studies. There are a limited number of sections in each of the cardinal planes, and there are large gaps between the sections. A further critical limiting factor of the Angevine and other atlases is that the cerebellum is not viewed within the widely used proportional stereotaxic space of Talairach and Tournoux. It is therefore not possible to determine the anatomic correlate of a Talairach coordinate derived from a functional imaging experiment. Even coregistration of a PET image with an MRI template of the cerebellum may not produce precise structure–function correlations because there is no atlas that can accurately identify the activated anatomic structure.

An additional consideration that limits the useful-

1053-8119/99 $30.00

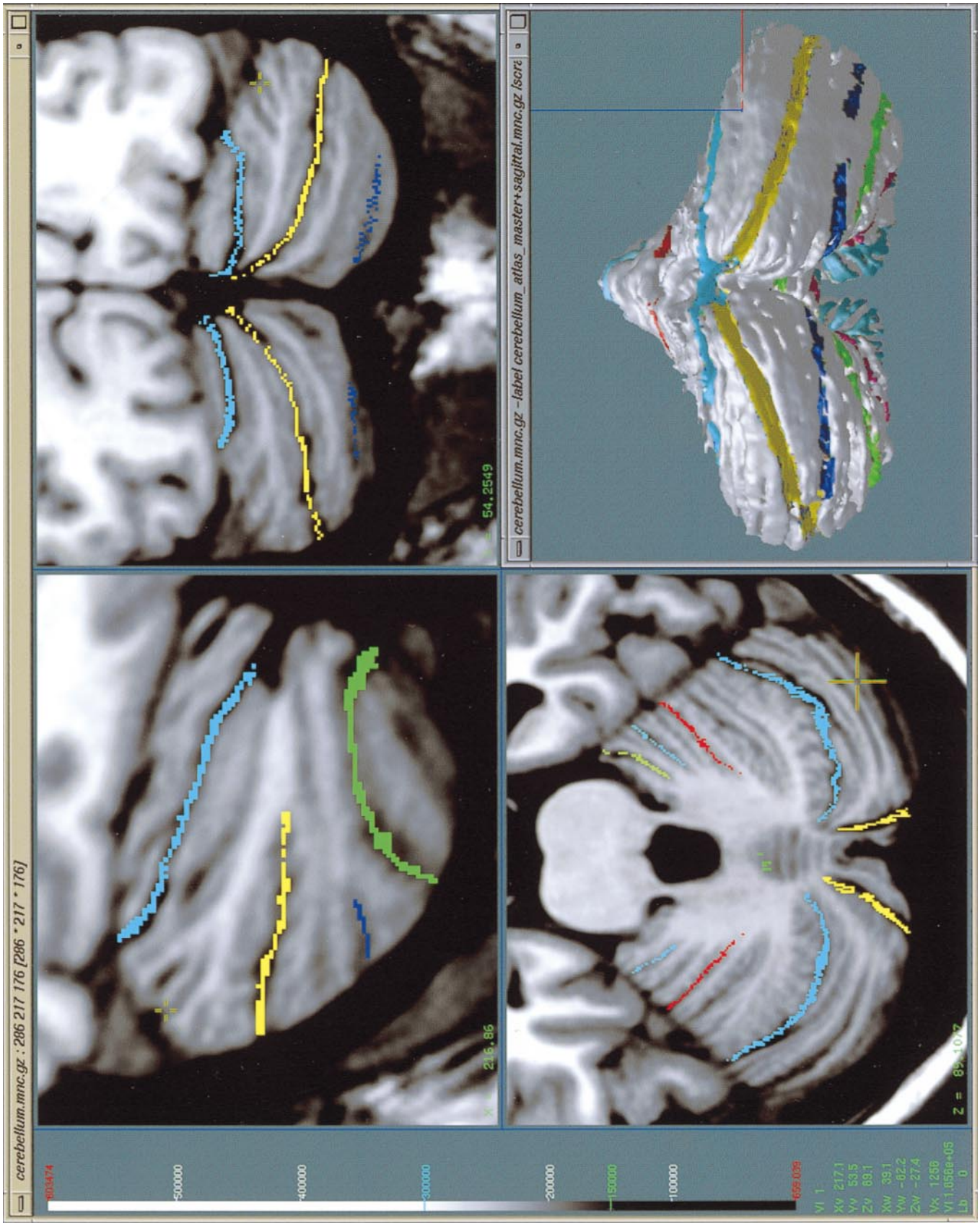
cerebellum.mnc.gz : 286 217 176 [286 * 217 * 176]
cerebellum.mnc.gz -label cerebellum_atlas_master+sagittal.mnc.gz
Z = 54.2549
Z = 89.1012

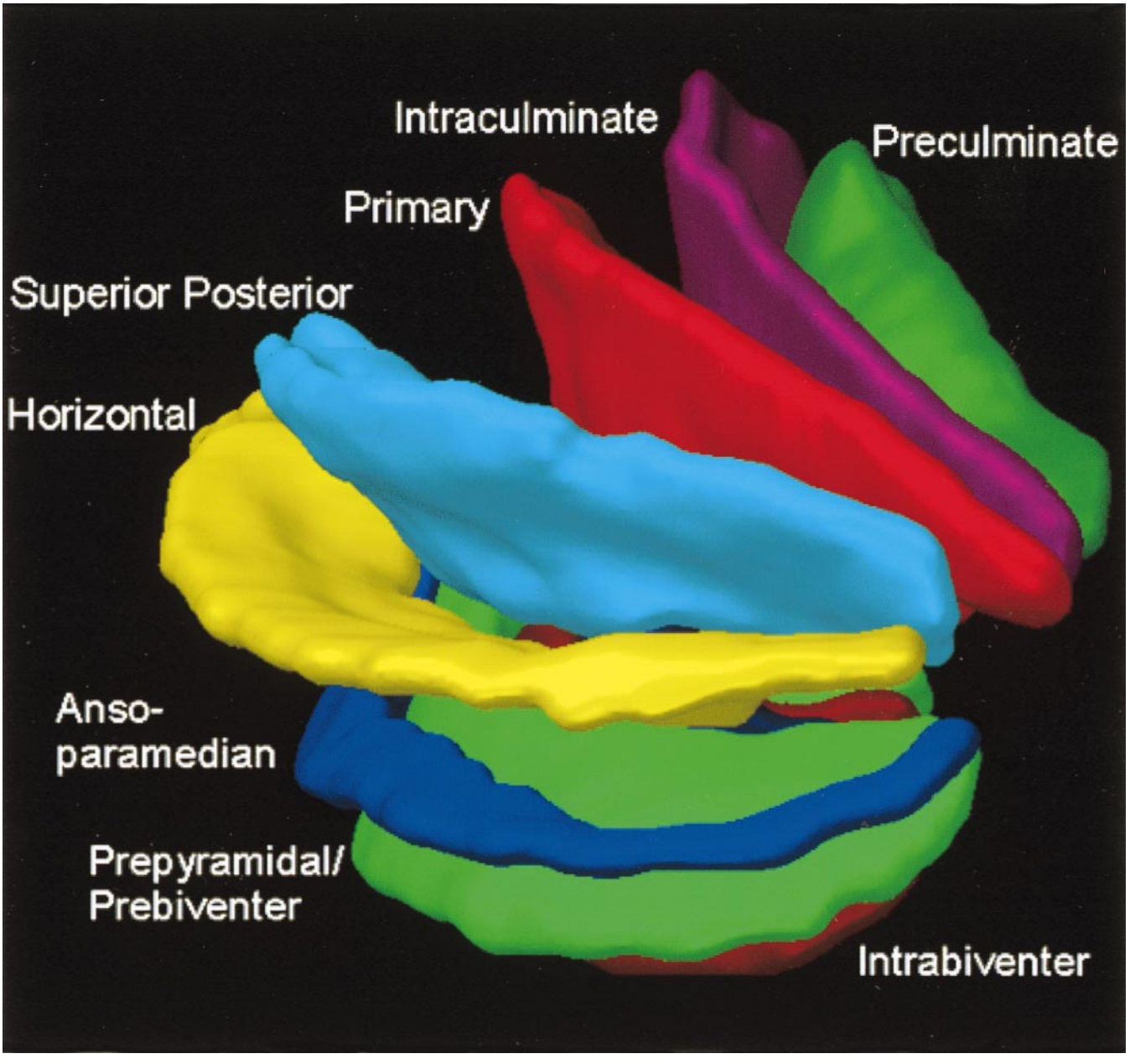

FIG. 2. Right lateral view of the fissures with cerebellar tissue removed.

ness of available atlases is that the terminology used to identify the fissures and lobules is not uniform and is often contradictory. There have been many revisions of the nomenclature of cerebellum of both human and monkey through the years (Malacarne, 1776; Vicq d' Azyr, 1786; Meckel, 1838; His, 1895; Stroud, 1895; Flatau and Jacobsohn, 1899; Dejerine, 1901; Smith, 1902; Bradley, 1904; Bolk, 1906; Edinger, 1909; Ingvar, 1918, 1928; Langelaan, 1919; Jakob, 1928; Riley, 1929, 1930; Anatomical Society of Great Britain and Ireland, 1933; Ziehen, 1934; Ariëns Kappers *et al.*, 1936; Dow, 1942; Loyning and Jansen, 1955; International Anatomical Nomenclature Committee, 1956; Jansen and Brodal, 1958; Larsell 1934, 1937, 1947, 1953, 1958, 1962, 1970; Larsell and Jansen, 1972). The number of attempts to understand the gross morphologic organiza-

FIG. 1. This figure illustrates the Display software used in this study. The cursor is visible on the sagittal, coronal, and axial views of the cerebellum as well as on a 3-D reconstruction of the surface.

tion of the cerebellum reflects the difficulty of the task. There is considerable variation and conflict within the terminologies previously adopted. The activation seen in functional imaging studies and the precision with which MRI can determine the site of a lesion in the human cerebellum make it imperative now that each region be identified by a uniform nomenclature. It is also important to correlate hemispheric and vermal components of each lobule and to compare human cerebellar morphology with that of lower species (Larsell, 1970; Madigan and Carpenter, 1971).

A detailed atlas developed specifically for use in conjunction with anatomic and functional neuroimaging would be a valuable tool for understanding the human cerebellum. This is essential in order to address questions of functional localization, the predictability of location of cerebellar fissures, lobules, and folia, and the possibility of predictable asymmetry across the hemispheres. The difficulty in correlating the details of focal activations in functional imaging studies with only vague notions of cerebellar anatomy has hampered the understanding of the human cerebellum and of how it is incorporated into the distributed neural circuits that subserve different domains of neurologic function.

We have therefore prepared a human cerebellar atlas using high-resolution MRI images that satisfies many of the mandates of a useful atlas. It is presented in the three cardinal planes in a universally understood system of proportional stereotaxic space with sections shown at 2-mm intervals, displaying high resolution, and utilizing a revised and simplified nomenclature that avoids the terminological confusion that characterized earlier attempts. This paper presents the methodology used, selected sections of the atlas, and 3-dimensional depictions of the lobules and fissures. We also present a revised nomenclature developed from this atlas.

METHODS

Magnetic Resonance Imaging

A signal-enhanced magnetic resonance (MR) scan was used to permit the identification of brain structures in as noise-free data as possible. To produce these images, a series of 27 T1-weighted MR scans was obtained from a single subject (CJH) using a Phillips 1.5 Tesla MR. The scan parameters were: 3D sagittal volume composed of 140 1-mm slices, FOV 256 mm (SI) $\times$ 204 mm (AP), acquired with a spoiled GRASS (TR/TE = 18/10 ms, flip angle 30°, NSA (NEX) 1, flow compensation on for a total scan time of 10 h 50 min, during 27 scans. The 27 scans consisted of 20 1.0-mm^3 vol and 7 0.78-mm^3 vol. The scans were acquired over a period of 3 months, with the maximum duration of any scanning session being 3 h. Each scan was registered and transformed into a standard proportional stereotaxic space, the Montreal Neurologic Institute (MNI) 305 brain averaged-space (Talairach and Tournoux, 1988), using an automatic registration tool (Collins *et al.*, 1994) and resampled to 0.5 mm^3 before normalization and intensity averaging. The effect of the intensity averaging of the 27 vol was a gain of approximately 4.5 in the signal-to-noise ratio. This effect was accentuated by the reduction of partial volume effects. Due to the unavoidable small motions of the head between scans, each region of space was imaged in slightly different voxels in each scan. As the final point sample was drawn from many volumes, all slightly displaced with respect to one another, the final subsampled voxels reduce the overall partial volume effect. Further details of the production of the intensity average of these volumes have been reported previously (Holmes *et al.*, 1998).

Identification of Cerebellar Fissures and Lobules

The brain slices were viewed using in-house software of the McConnell Brain Imaging Center running on Silicon Graphics workstations (Fig. 1). The interactive portion of the software, Display, provided several simultaneous views of imaging data, including sagittal, coronal, and horizontal cross-sections. Within each view a variety of standard color-coding algorithms was invoked to assign colors to the numerical values of the images, and each view could be independently magnified and translated. The current positions of the cross-sectional planes were chosen by selecting a point on any view that caused the positions of the other views to change accordingly. This permitted cross-correlation of a given locus between the different planes. Individual voxels in the image volume were labeled with an arbitrary integer label by using the mouse to sweep out a circular brush across an image plane. In addition, a three-dimensional view of reconstructed surface geometry was available. The boundaries in an image or labeling of an image were created by an isosurface triangulation algorithm (Lorenson and Cline, 1987) and displayed in the three-dimensional window.

The atlas of Angevine *et al.* (1961) was used to identify fissures that could reliably be seen on the midsagittal plane. The cerebellar fissures were then identified by labeling empty voxels in the center of each fissure on every slice in all three planes, and this information was used to parcellate the lobules and folia. For those fissures that were optimally seen on more lateral sections (e.g., the superior posterior fissure), comparison was made with corresponding parasagittal sections in the atlas of Angevine *et al.* and validated using the coronal and horizontal images of this atlas.

The voxellated fissures were subjected to a least-squares curve-fitting smoothing algorithm, which assisted in the final stage of presentation of the data. The images were rendered with in-house ray-tracing soft-

ware with appropriate ruled indicators delineating positions in Talairach space. Finally, the lobules were labeled according to our revision of the cerebellar nomenclature that respects the vermal–hemispheric correlation outlined in Table 1 and explained further below.

This investigation was not specifically designed to study the detailed anatomy of the deep cerebellar nuclei. The outline of the nuclei characterized by the gray-white matter differentiation proved indistinct on these images. It was therefore difficult to define their limits with certainty. This was true for the nuclei as a group, as well as for the delineation of the fastigial, globose, emboliform, and dentate nuclei from each other. This limitation was compensated for by comparison with postmortem cryosections of another cerebellum. This cryosectioned brain was prepared, digitized, and then warped into Talairach space as described elsewhere (Toga *et al.*, 1997). Equivalent sections in the cardinal planes were selected for comparison with the MRI atlas. The anatomy of the deep nuclei is well defined in these cryosections, and their location and configuration can be compared with the predicted location within the cerebellar parenchyma on the MRI images.

TABLE 1

Relationship of the Fissures to the Cerebellar Lobules in the Vermis and Hemispheres

VERMIS Lobule	FISSURE	HEMISPHERE Lobule
I,II		I,II
	Precentral	
III		III
	Preculminate	
IV		IV
	Intraculminate	
V		V
	Primary	
VI		VI
	Superior Posterior	
VIIAf		Crus I
	Horizontal	
VIIAt		Crus II
	Ansoparamedian	
VIIB		VIIB
	Prepyramidal /Prebiventer	
VIIIA		VIIIA
	Intrabiventer	
VIIIB		VIIIB
	Secondary	
IX		IX
	Posterolateral	
X		X

Three-Dimensional Reconstructions

The fissures marked on the serial sections were transformed into smooth sheets coursing through 3-dimensional space with the cerebellar tissue removed, using image blurring and the isosurface algorithm. Each set of labeled voxels was first blurred with a 5-mm-width box filter, then the isosurface algorithm was applied to the blurred image (Lorenson and Cline, 1987). The resulting triangulated surface constituted a visually smooth representation of the volumes of the fissures. These fissures suspended in the invisible cerebellum are shown as viewed from the right lateral aspect (Fig. 2). The external surface of the cerebellum was reconstructed by applying the isosurface algorithm to the average MR image. The surface markings of the fissures were identified on these views, and the cerebellum thus parcellated into lobules (Fig. 3).

Methodological Limitations

Single subject. There are important limitations that arise from the use of single brain to develop a cerebellar atlas. A number of variables are by definition excluded from consideration. It is not possible, for example, to evaluate consistency of hemispheric asymmetry and the individual variation of the size, shape, and constituent elements of an individual lobule. Some possible confounding variables such as gender, age, and handedness are also not factored into this evaluation. The utility of the approach used in this in-depth analysis of a single brain, however, is that the primary step is the identification of the major fissures, and the determination of the lobules and folia follows from this first step. The anatomic location of major fissures can be ascertained in other cerebella by reference to the anatomic features of this atlas, even if there is some variability in their location within standard stereotaxic space and some divergence from the exact shape of this particular cerebellum. This atlas can be used as the template for future population-based probabilistic studies that examine large numbers of cerebella, and that can address questions of individual variability determined by, or concomitant with, such considerations as gender and handedness. Morphometric studies of the cerebellum will also be facilitated by reference to the fissures, lobules, and folia demonstrated in this atlas. It is not possible to proceed to the next stage of morphologic studies of the cerebellum without first identifying the boundaries and structures of a single cerebellum using the MRI technology.

Talairach coordinate space. It could be argued that the use of Talairach proportional space is suboptimal for an atlas of the cerebellum because the anterior–posterior commissure line is far removed from the

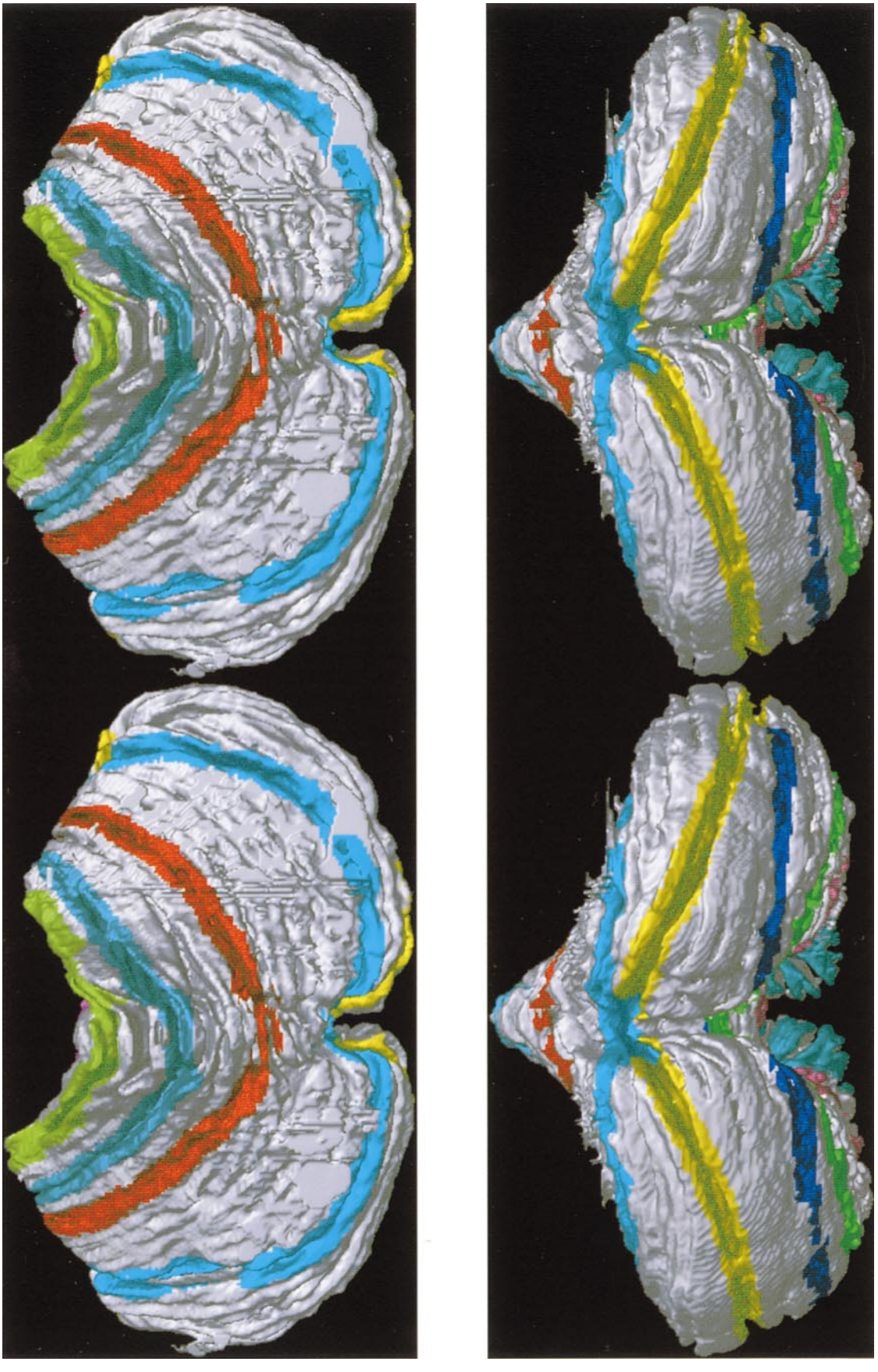

FIG. 3. 3-dimensional reconstructions of the superior (above) and posterior (below) surfaces of the cerebellum presented as stereo-pairs.

TABLE 2

Comparison of Earlier Nomenclature Systems with the Designation Used in This Atlas (Based on Larsell)

<table>
<tr><th>Schmahmann et al. (1999)</th><th>Consensus</th><th>Dejerine (1901)</th><th>Bolk (1906)</th><th>Ingvar (1918, 1928)</th><th>Riley (1929)</th><th>Larsell (1936-1972)</th></tr>
<tr><td>I,II</td><td>lingula</td><td>lingula</td><td>1</td><td>lingula</td><td>lobulus I vermalis</td><td>I, II
lingula</td></tr>
<tr><td>III</td><td>centralis</td><td>central</td><td>2</td><td>centralis</td><td>lobulus II vermalis</td><td>III
centralis</td></tr>
<tr><td>IV</td><td rowspan="2">culmen
[culmen of monticulus; culminis]</td><td rowspan="2">culmen</td><td>3</td><td rowspan="2">culmen</td><td rowspan="2">lobulus IV vermalis</td><td>IV
culmen</td></tr>
<tr><td>V</td><td>4</td><td>V
culmen</td></tr>
<tr><td>VI</td><td>declive
[declive of monticulus; clivus monticuli; lobulus clivi]</td><td>déclive</td><td>lobulus simplex</td><td>simplex</td><td>lobulus C2 vermalis, pre-sulcal</td><td>VI
declive</td></tr>
<tr><td>VIIAf</td><td>folium
[folium of vermis; folium cacuminis]</td><td>bourgeon terminal</td><td rowspan="3">C_2</td><td>lobulus medius</td><td rowspan="3">lobulus C2 vermalis, post-sulcal</td><td rowspan="2">VIIA
folium/tuber</td></tr>
<tr><td>VIIAt</td><td>tuber
[tuber of vermis; tuber valvulae]</td><td rowspan="2">tubercule valvulaire</td><td rowspan="2">medianus</td></tr>
<tr><td>VIIB</td><td>caudal aspect of tuber valvulae</td><td>VIIB
caudal aspect of tuber</td></tr>
<tr><td>VIIIA</td><td rowspan="2">pyramis</td><td rowspan="2">pyramide</td><td rowspan="2">C_1</td><td rowspan="2">pyramis</td><td rowspan="2">lobulus C1 vermalis</td><td>VIIIA
pyramis</td></tr>
<tr><td>VIIIB</td><td>VIIIB
pyramis</td></tr>
<tr><td>IX</td><td>uvula</td><td>luette</td><td>b</td><td>uvula</td><td>lobulus B vermalis</td><td>IX
uvula</td></tr>
<tr><td>X</td><td>nodulus</td><td>nodule</td><td>a</td><td>nodulus</td><td>lobulus A vermalis</td><td>X
nodulus</td></tr>
</table>

posterior fossa. The concern, therefore, is that the margin of error in reporting the location of structures (or structure–function correlations) in cerebellum is unacceptably great. This concern may have validity, but the Talairach system is widely used, and activations on functional imaging scans are commonly reported in both cerebral and cerebellar structures using the same sagittal/coronal/axial images. It seems possible to develop a system of coordinates specifically for use with the posterior fossa, but the overall utility of this approach may be less generally applicable. The degree to which the location of the cerebellar folia are

TABLE 2—*Continued*

Schmahmann et al. (1999)	Henle (1879)	Schwalbe (1881)	Kuithan (1895)	BNA (1895)	Flateau & Jacobson (1899)	Dejerine (1901)	Smith (1902)	Bolk (1906)	Schäfer & Symington (1908)	Ingvar (1918, 1928)	Langelaan (1919)	Riley (1929)	BNA-BR (1933)	Ziehen (1934)	Ariëns Kappers et al. (1936)	Dow (1942)	NAP (1955)	Jansen & Brodal (1958)	Larsell (1936-72)	Angevine et al. (1961)	Press et al. (1989)
I,II	vinculum lingulae	frenulum lingulae	lingula	vinculum lingulae cerebelli	lingula	frein de la lingula	lingula	I	fraenulum lingulae	lingula	lobus vinculo-lingualis	lobulus I lateralis	lingula	vinculum lingulae	lingula	lingula	lingula cerebelli	lobulus I	H II lingula	lingula	lingula
III	lobus centralis	lobus centralis	ala lobuli centralis	ala lobuli centralis	ala lobuli centralis	aile du lobule central	pars preculmi-nata	2	ala lobuli centralis	centralis	lobus centro-alaris	lobulus II lateralis	ala lobuli centralis	ala lobuli centralis	ala lobuli centralis	lobulus centralis	ala lobuli centralis	lobulus centralis, II, III	H III centralis	lobulus centralis	central lobule
IV	lobus quadran-gularis	lobus lunatus anterior	lobus lunatus anterior	lobulus quadran-gularis, pars anterior	lobulus quadrang-ularis	partie antérieure du lobe quad-rilatère	pars culminus (pars culminata)	3	lobulus lunatus anterior	culmen	lobus culmino-lunatus	lobulus IV lateralis	lobulus lunatus anterior	lobus quadran-gularis, pars anterior	lobus quadri-laterus anterior	culmen	lobus quadran-gularis	lobulus quadran-gularis anterior	H IV culmen H V	culmen	quadran-gular lobule, anterior portion
V								4													
VI		lobus lunatus posterior	lobus lunatus posterior	lobulus quadrang-ularis, pars posterior		partie postérieure du lobe quad-rilatère	area lunata	lobulus simplex	lobulus lunatus posterior	lobulus simplex	lobus declivo-lunatus	lobulus ansiformis, crus 1	lobulus lunatus posterior	lobus quadran-gularis, pars postrerior	lobus quadri-laterus posterior	lobulus simplex	lobulus simplex	lobulus quadran-gularis posterior	H VI lobulus simplex	lobus simplex	quadran-gular lobule, posterior portion
Crus I	lobus semi-lunaris superior	lobus posterior superior	lobus semi-lunaris superior	lobulus semi-lunaris superior	lobulus semi-lunaris superior	lobe semi-lunaire supérior	area pteroidea	lobulus ansiformis, crus I	lobulus posterior superior	lobulus ansiformis	lobus folio-semi-lunaris		lobulus ansiformis, facies superior	lobulus semi-lunaris superior	lobus semi-lunaris superior	crus I of lobulus ansiformis	lobulus semi-lunaris superior	lobulus semi-lunaris superior	crus I of H VIIA/ lobuli ansiformis	crus I, lobulus ansiformis	semilunar lobule, superior portion
Crus II	lobus semi-lunaris inferior	lobus posterior inferior	lobus semi-lunaris inferior	lobulus semi-lunaris inferior	lobulus semi-lunaris inferior	lobe semi-lunaire inférieur	area post-pteroidea	lobulus ansiformis, crus II	lobulus semi-lunaris inferior		lobus tubero-semi-lunaris	lobulus ansiformis, crus 2	lobulus ansiformis, facies inferior	lobulus semi-lunaris inferior	lobus semi-lunaris inferior		lobulus semi-lunaris inferior	lobulus semi-lunaris inferior	crus II of H VIIA/ lobuli ansiformis	crus II, lobulus ansiformis	semilunar lobule, inferior portion
VIIB				lobulus gracilis		lobe grêle			lobulus gracilis						gracilis			lobulus gracilis	H VIIB lobulus para-medianus	lobulus para-medianus	gracile lobule
VIIIA	biventer	lobus cu-neiformis sive biventer	lobus cu-neiformis	lobulus biventer	lobulus biventer	lobe digastrique	area para-pyrami-dalis	lobulus para-medianus	lobulus biventralis		lobus pyramido-biventricus	lobulus para-medianus		lobulus biventer (2 parts)	crus secundum lobi ansiformis	crus II lobulus ansiformis	lobulus biventer	lobulus biventer/ parfloc-culus dorsalis	H VIIIA lobulus biventer, pars copularis	lobulus biventer, pars copularis	biventer
VIIIB																			H VIIIB l. biventer, pars para-flocculus dorsalis	lobulus biventer, pars para-flocculus dorsalis	
IX	tonsilla	tonsil	tonsil	tonsil	tonsil	amygdale		crus circum-cludens	tonsil	lobulus para-medianus/ tonsil	lobus uvulo-tonsillaris	lobulus para-flocc ularis	tonsilla	tonsilla	lobus para-medianus (tonsilla)	lobulus para-medianus	tonsilla	tonsilla/ para-flocculus ventralis	para-flocculus ventralis	para-flocculus	tonsil
X	flocculus	flocculus	nodulus	flocculus	flocculus	floculus	flocculus	pars floccularis	flocculus	flocculus	lobus nodulo-floccularis	lobulus floccularis	flocculus	flocculus	flocculus	flocculus	flocculus	flocculus	flocculus	flocculus	flocculus

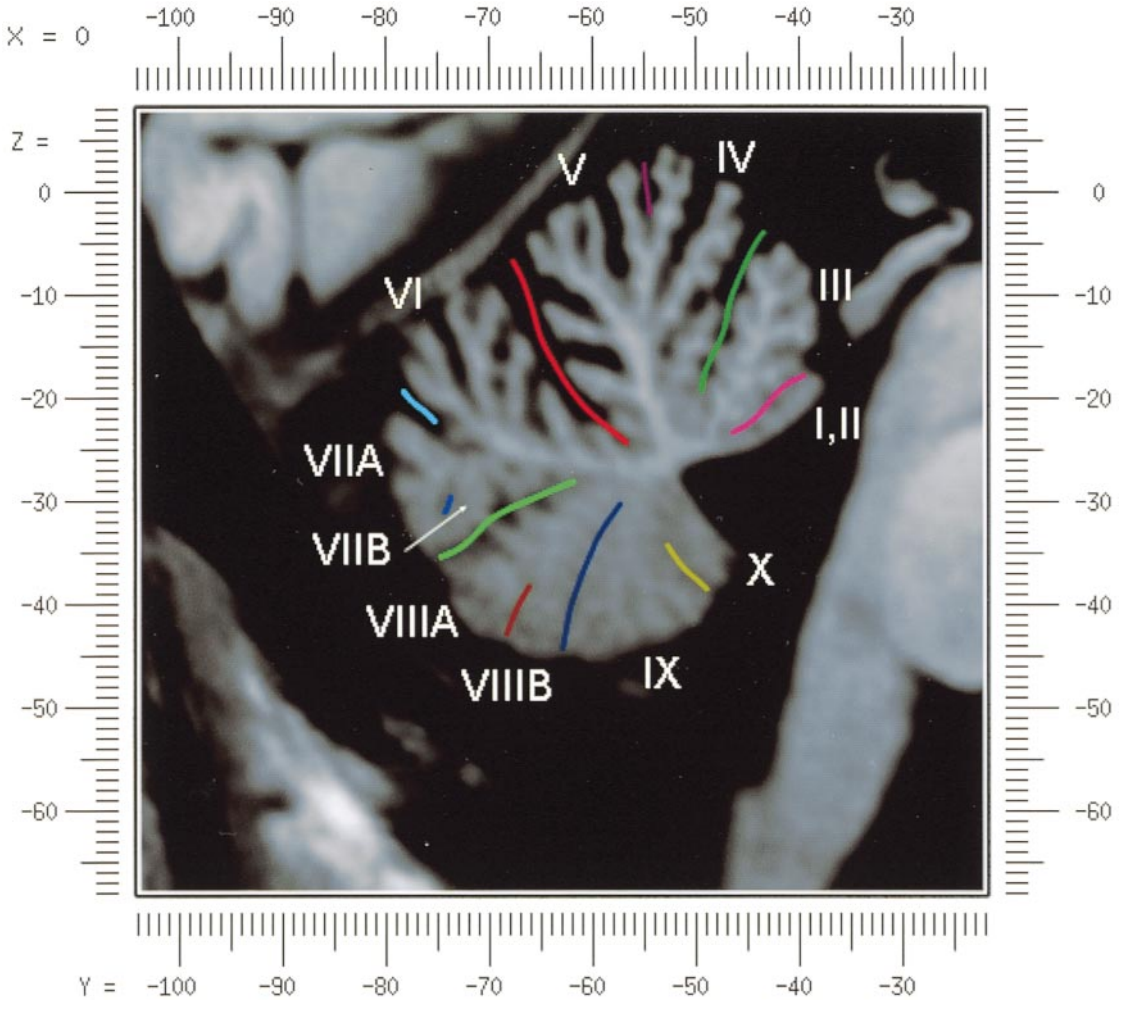

FIGS. 4–14. Sagittal images of the right cerebellum (Figs. 5–9) and left cerebellum (Figs. 10–14), progressing laterally by increments of 10 mm. The midsagittal plane ($x = 0$) is shown in Fig. 4. In this and subsequent figures, the fissures are color coded according to the convention in Table 1.

consistent from one brain to the next using this stereotaxic proportional space will need to be determined in future investigations.

Cerebellar nuclei. The absence of clearly visible boundaries of the cerebellar nuclei on the MRI prevented the confident incorporation of the nuclei into this atlas. This limitation was partially overcome by comparison with digitized autopsy cryosections of cerebellum warped into Talairach space.

Nomenclature

What began as a straightforward project of mapping the fissures and the nomenclature used by Angevine *et al.* (1961) onto the MRI images turned out to be more complicated. The nomenclature systems used by both early and contemporary investigators are confusing. We addressed this issue by reviewing the evidence in support of the different terminologies presented by the investigators mentioned above, starting with that of Vincenzo Malacarne in 1776. The atlas of Angevine *et al.* also helped us revise the nomenclature and determine the relationship between the fissures and lobules, because their atlas included an analysis, comparison, and synthesis of the findings of many of the earlier investigators. By using the current technology (MRI reconstructions and Display software that permits simultaneous cross-referencing between the three planes) we were able to explain the origins of some terminological difficulties that have arisen over the past two centuries and then resolve them. We amended the terminology of Larsell and compared this with the terminologies introduced by Malacarne (1776), Bolk (1906), Ziehen (1934), and others. In so doing we adopted a nomenclature that is anatomically correct,

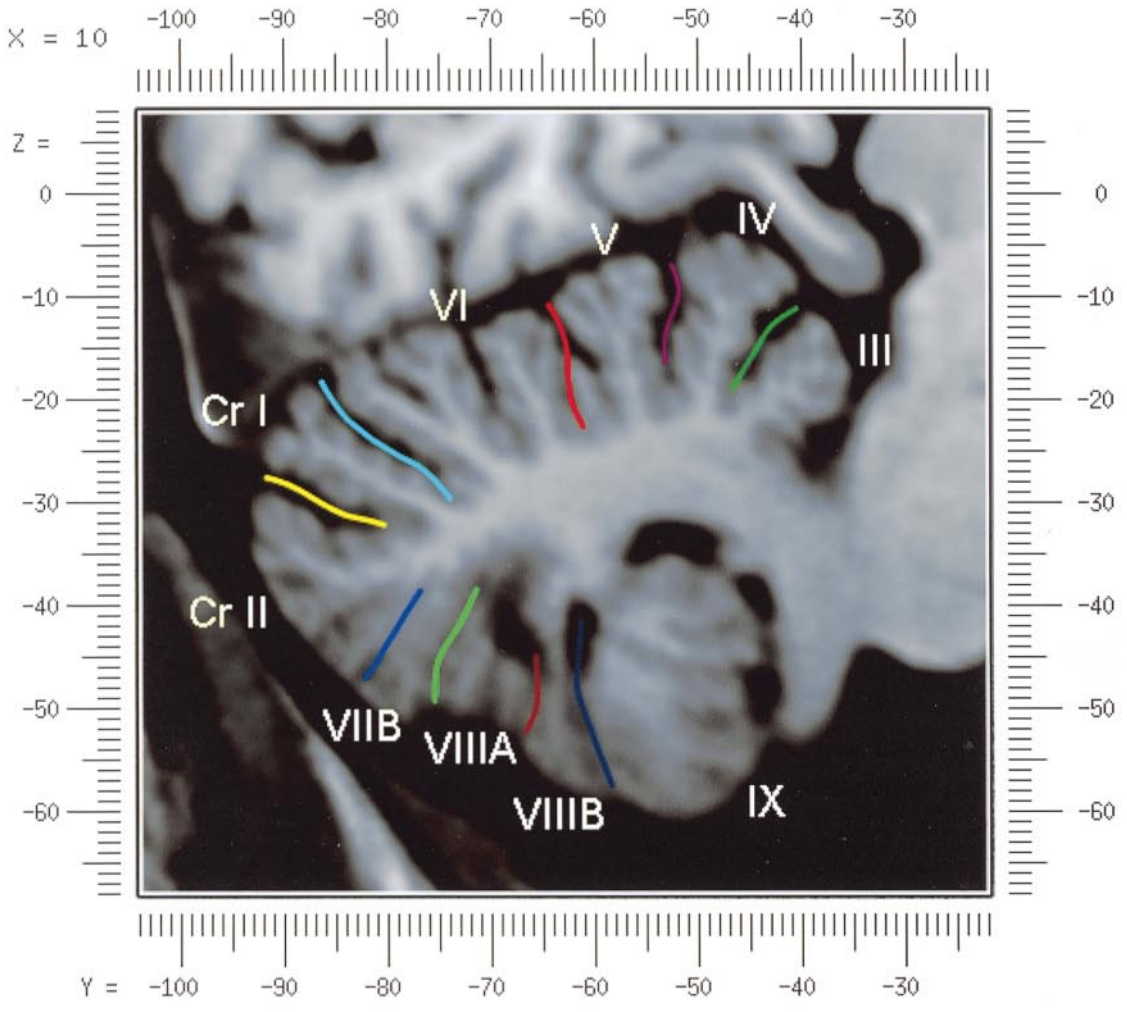

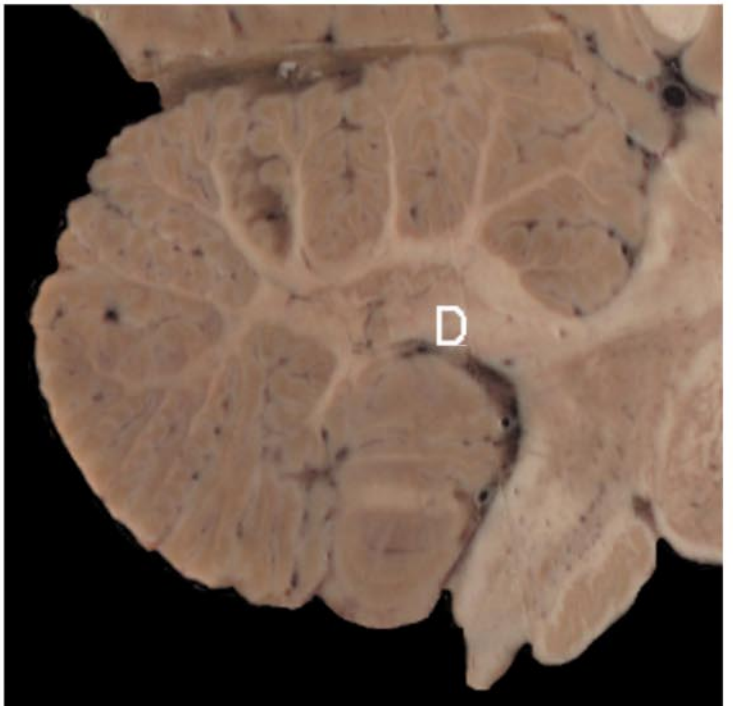

FIG. 5. Top: Sagittal MRI image of the cerebellum 10 mm to the right of midline. Bottom: A postmortem cryosection of another human cerebellum in the sagittal plane prepared according to the method of Toga et al. (1997), corresponding to $x = +10$ mm. D, dentate nucleus.

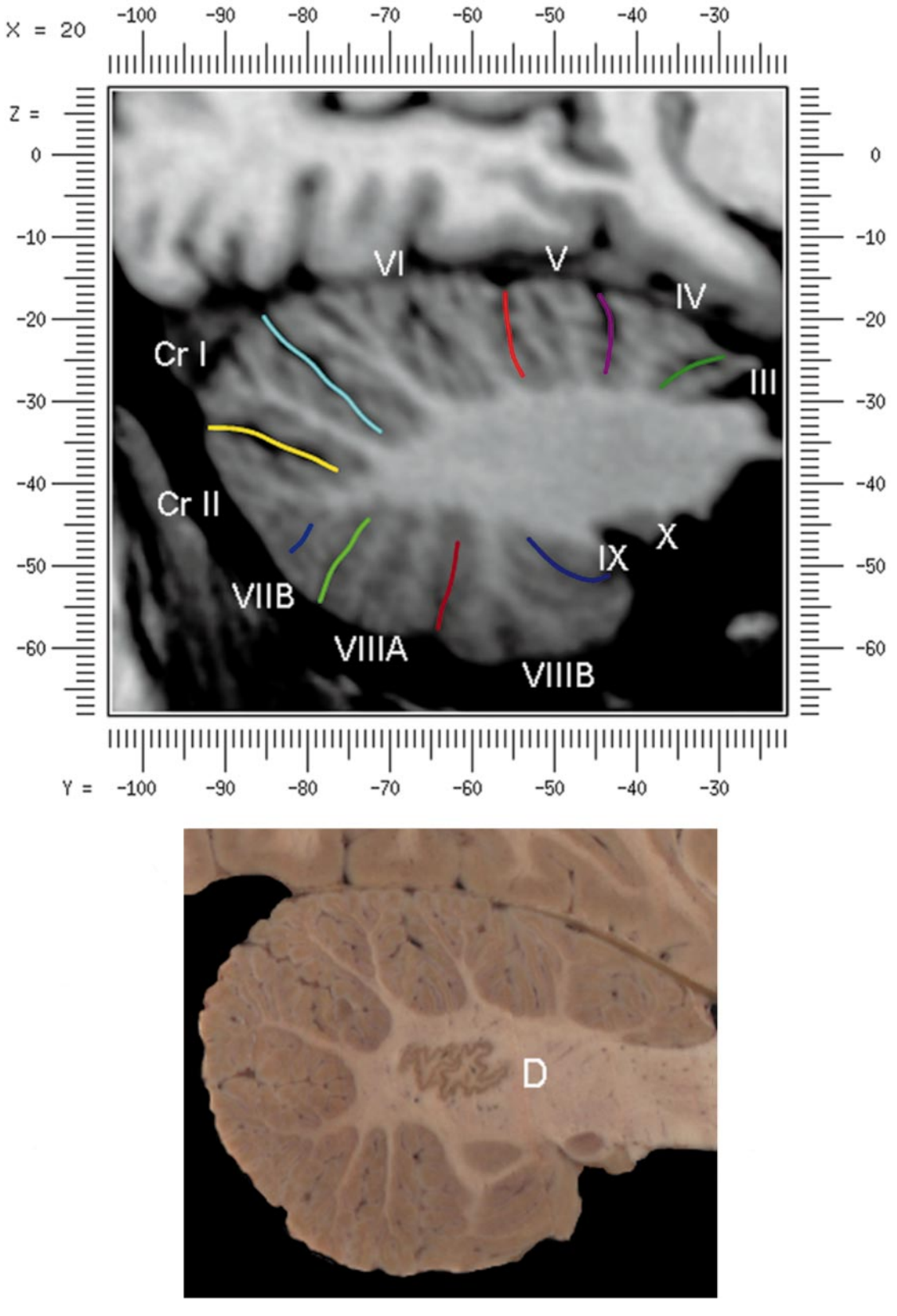

FIG. 6. Bottom: A cryosection in the sagittal plane corresponding to $x = +20$ mm. D, dentate nucleus.

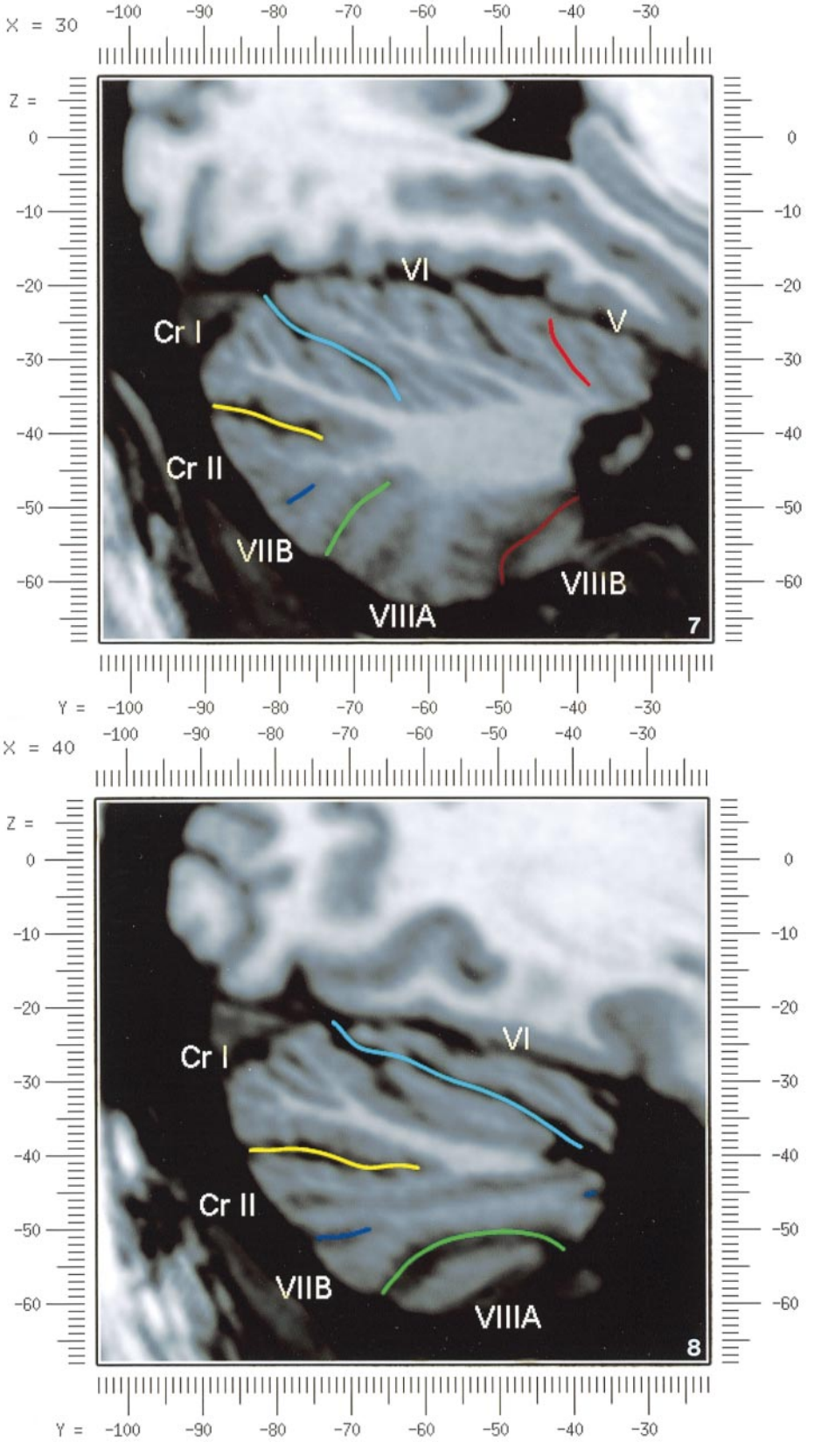

FIGURES 7 AND 8

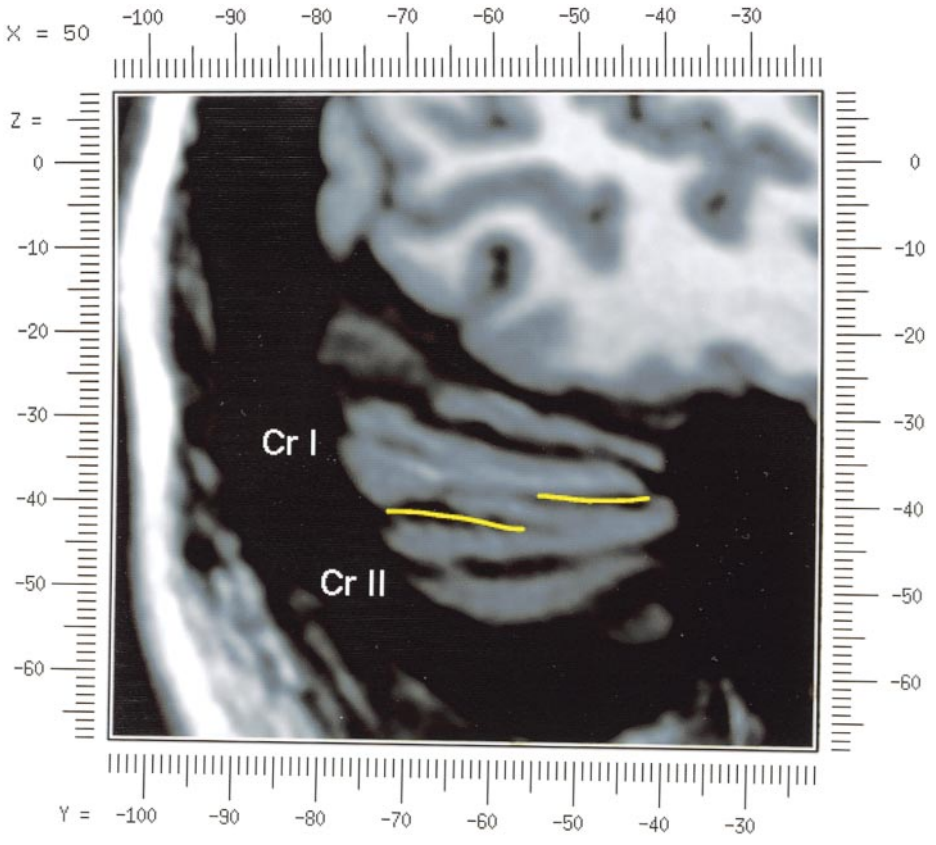

FIGURE 9

easily understandable, and melds with the neuronames brain hierarchy (Bowden and Martin, 1995) accepted by the International Consortium for Brain Mapping.

The method employed for determining the simplified nomenclature was derived from the use of the atlas itself. Vermal lobules were identified with the assistance of the midsagittal section of the Angevine atlas, subsequent to the identification of the fissures and sulci. The lobules that could be readily discerned in the hemisphere were also demarcated, such as crus I and crus II that are separated by the horizontal fissure that is prominent in lateral sections. By applying a slightly modified version of the Larsell (1970; Larsell and Jansen, 1972) terminology, and maintaining consistency through all planes in continuous adjacent 0.5-mm sections, it was possible to determine which folium belonged to which lobule and which Larsell designation was appropriate. The descriptions and illustrations of the rhesus monkey cerebellum by Larsell (1970) and Madigan and Carpenter (1971) were also helpful in furthering our understanding of the folia of the human cerebellum. Some of the small subfolia buried at the fundus of the fissures or sulci were troublesome, but most could be parcellated by use of the 3-dimensional correlations.

The Problem of the Vermis

There is no true "vermis" in the anterior lobe. The application of this term to the paramedian sectors of the anterior lobe is an extension of the Latin term (meaning worm) used by Malacarne to denote the structure visible in the posterior and inferior aspect of the cerebellum. The vermis (as such) is present from lobules VI through X. The use of the term vermis to indicate "midline" has become well entrenched, however, and in so doing it has brought with it the problem of defining what is the lateral extent of the anterior lobe "vermis." It has been suggested that the paravermian sulcus limits the vermis laterally. In many brains there is no paravermian sulcus and where one appears to be present, it may simply reflect the indentation produced by the course of the medial branch of the superior cerebellar artery. On coronal section the anterior lobe (lobules I through V) has cortex buried beneath the overlying midline cortex, separated from the hemispheral cortex by a superior white matter extension of the medullary core (see, e.g., coronal sections $y = -42$ through $y = -58$). Even where there may be a paravermian sulcus this is most likely the preculminate fissure (see coronal section $y = -42$) or the intraculminate fissure ($y = -48$) that is not necessarily constant from

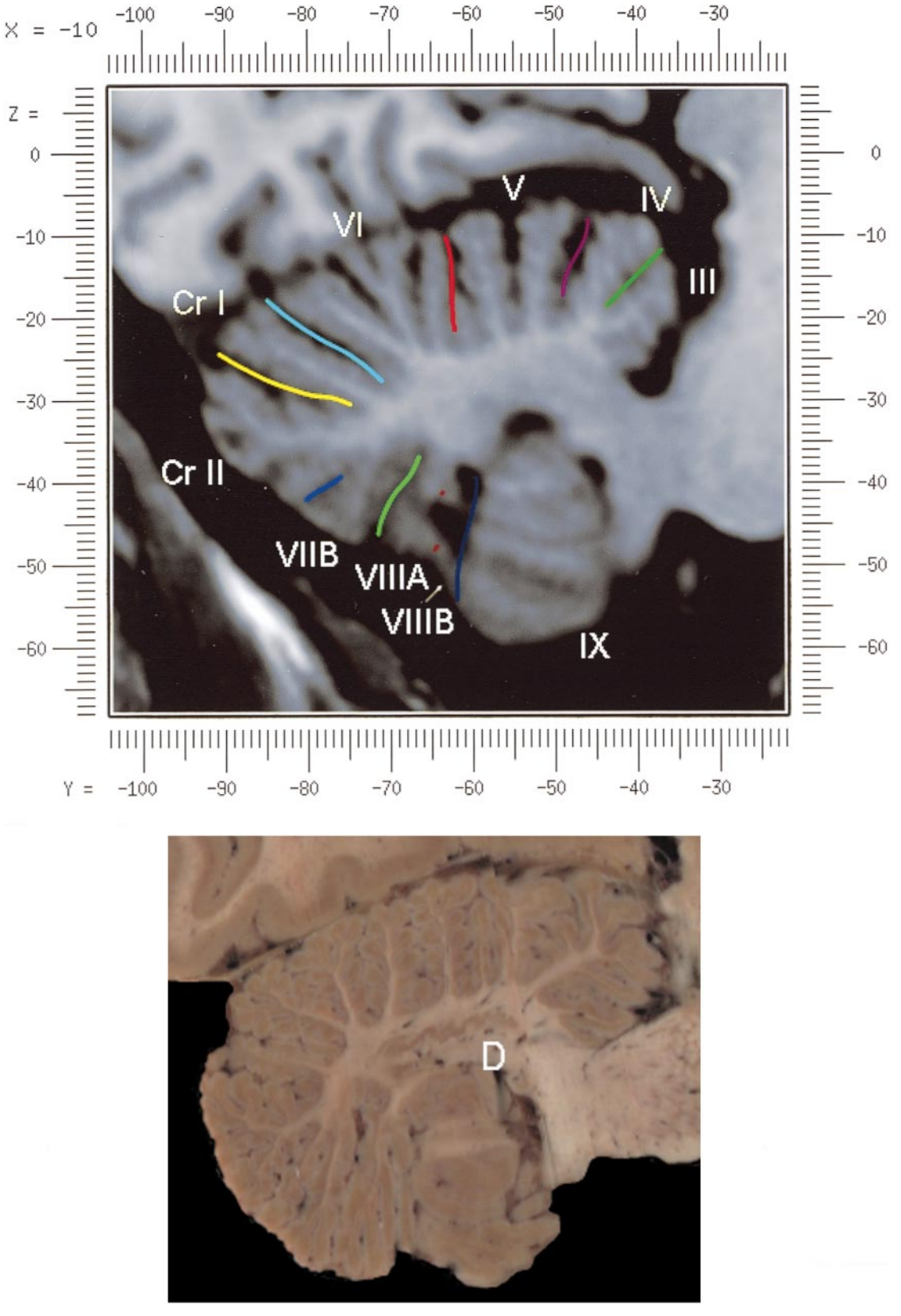

FIG. 10. Bottom: A cryosection in the sagittal plane corresponding to $x = -10$ mm. D, dentate nucleus.

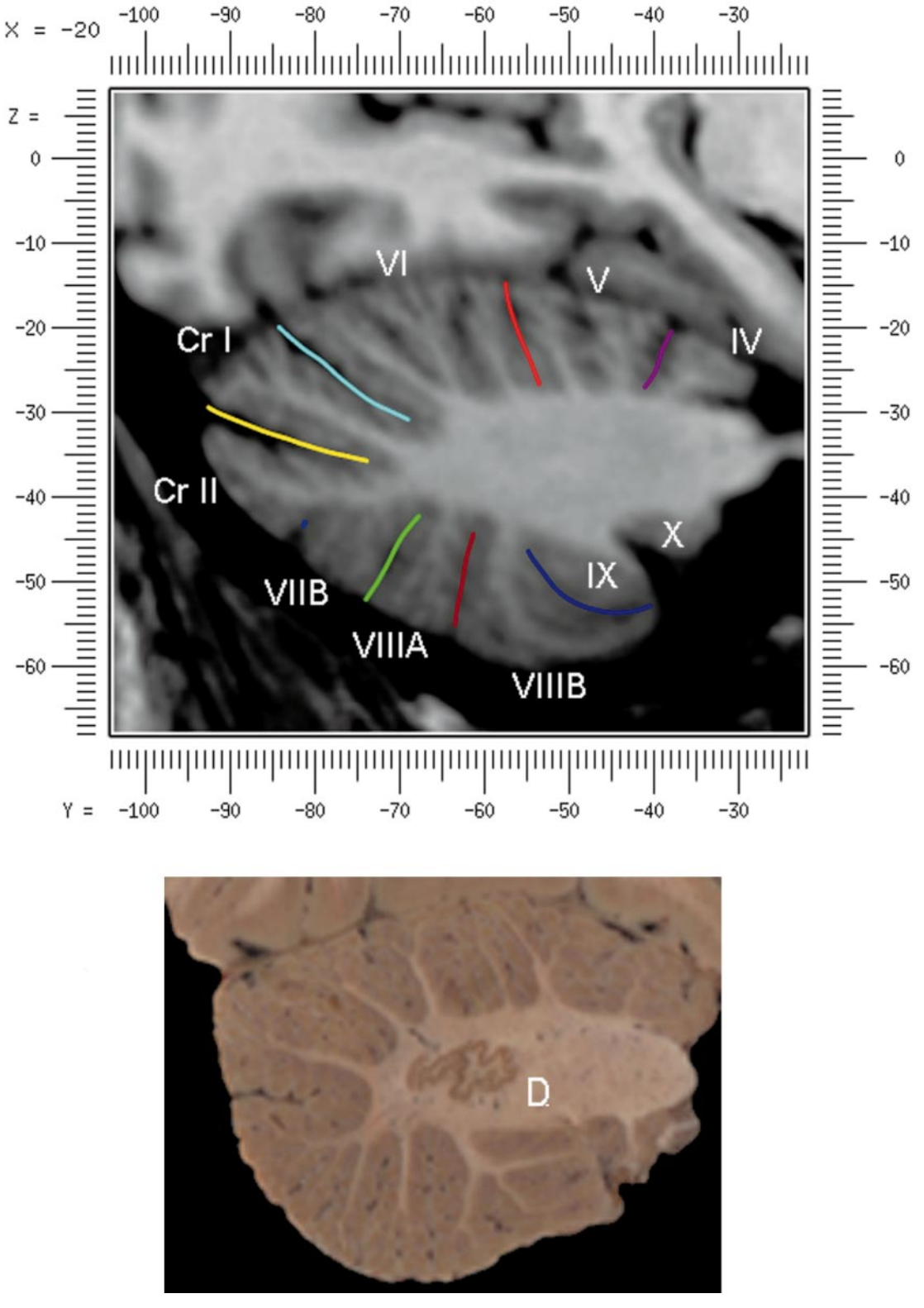

FIG. 11. Bottom: A cryosection in the sagittal plane corresponding to $x = -20$ mm. D, dentate nucleus.

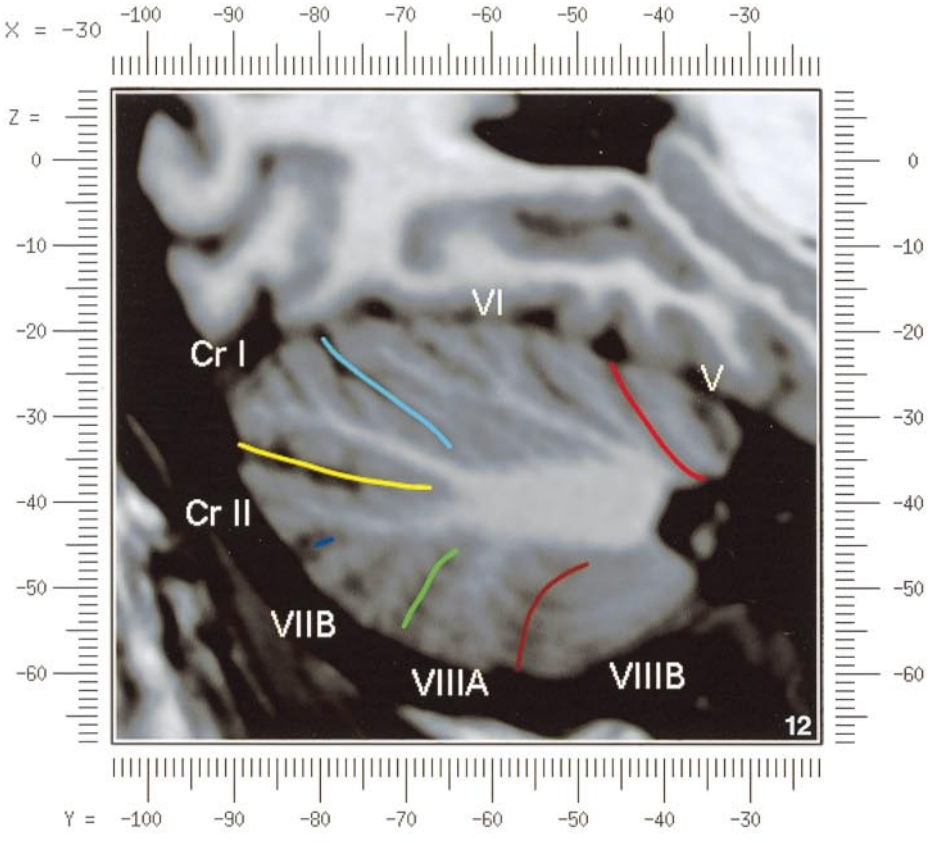

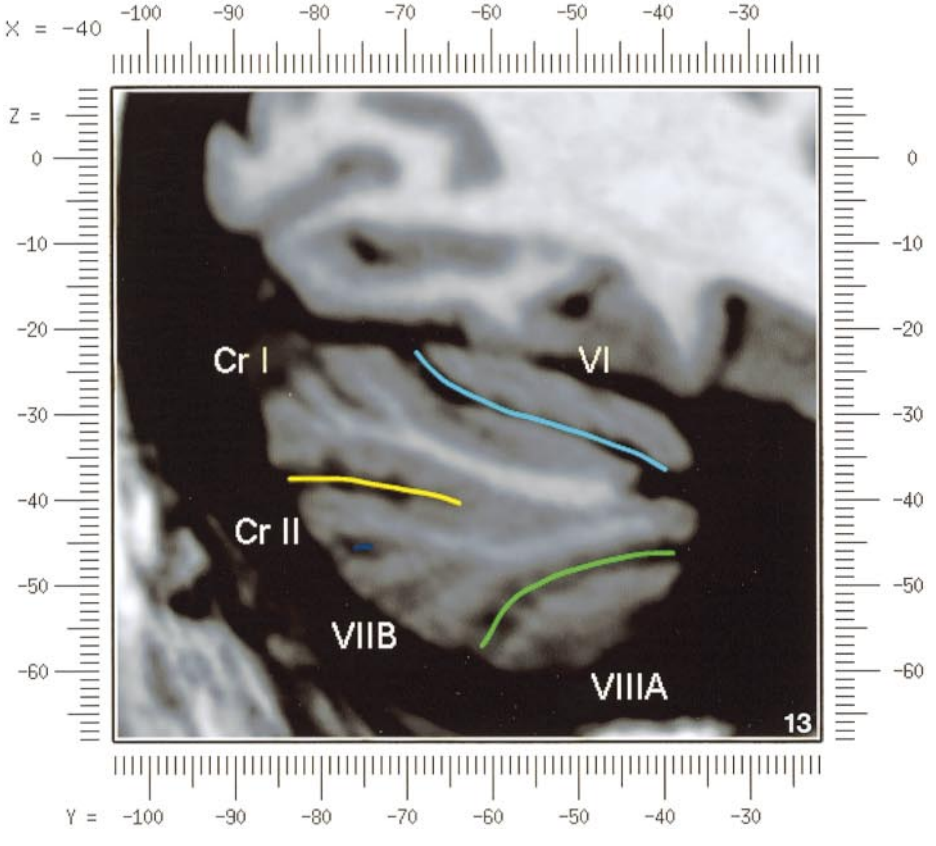

FIGURES 12 AND 13

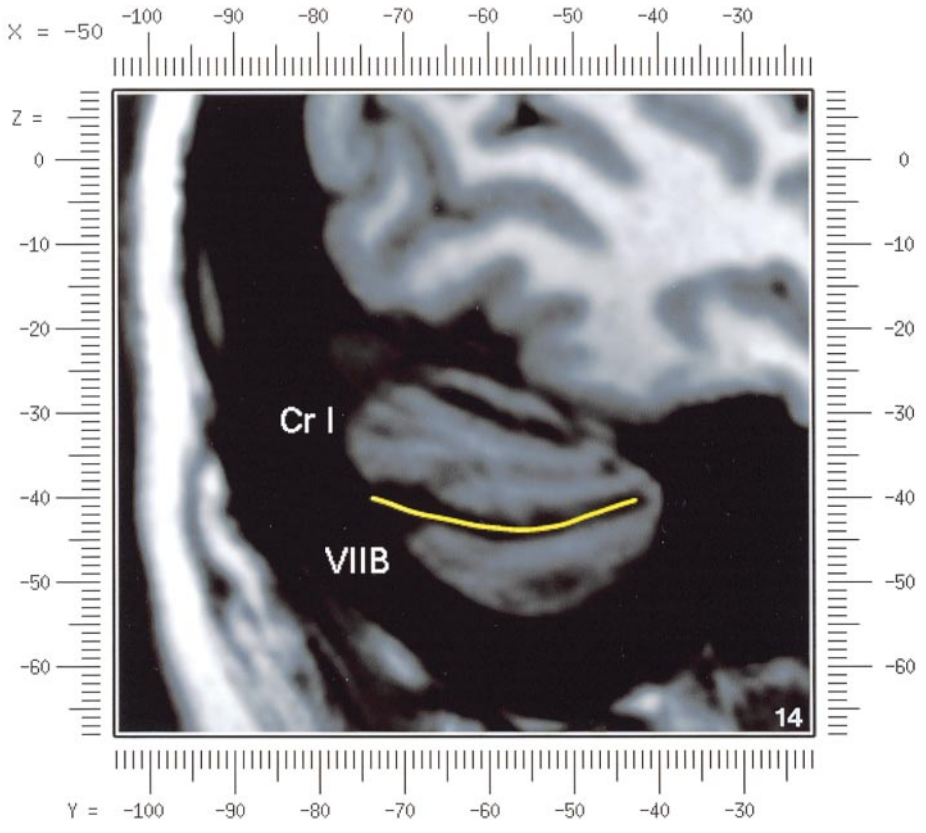

FIGURE 14

one section to the next and does not demarcate the lateral extent of the hidden cortex that truly occupies a midline position between the hemispheres. In this brain the anterior lobe "vermis" occupies a mediolateral extent that varies from 14 to 20 mm depending on the section and the definition of the lateral boundary (surface markings of the "paramedian sulcus"; lateral extent of the buried cortex; lateral aspect of the paramedian white matter laminae). Each brain will no doubt vary to some extent, and the functional significance of this distinction is not known. The determination of the lateral extent of the "vermis proper" (in the posterior lobe) is not a problem, as this is a gross morphologic term originally intended to define a structure visible on the surface of the brain.

Larsell distinguished the vermis from the hemispheral compartments of the different lobules by using the prefix "H" for the hemispheres. As the bulk of the cerebellum is composed of hemisphere, and the "H" designation adds a cumbersome element to the description of the lobules, we dispensed with this designation. Instead, when referring to a midline structure the term vermal area (anterior lobe) or vermis (posterior lobe) was added.

RESULTS

The technique of averaging multiple scans of the same brain produced MR images that were of high resolution and permitted detailed evaluation. The coregistration of the images in sagittal, coronal, and horizontal planes was an essential tool in the definition of both fissures and folia and facilitated the characterization of these structures with confidence. Eleven major fissures were identified, and these were used to subdivide the cerebellum into lobules. The 3-dimensional reconstruction of the surface of the MRI cerebellum with the superimposed externally visible fissures provided independent confirmation of the accuracy of the labeling of the fissures. The differentiation of folia and subfolia was clear in most instances. The cerebellar cortex could usually be distinguished from the medullary core and medullary rays extending into the larger folia. Cerebellar nuclei on the MRI images were visible as gray matter structures situated within the medullary core; however, they were not sufficiently well defined to permit accurate delineation. The nuclei were readily identifiable, however, on the equivalent sections derived from the cryosections of the postmortem human cerebellum.

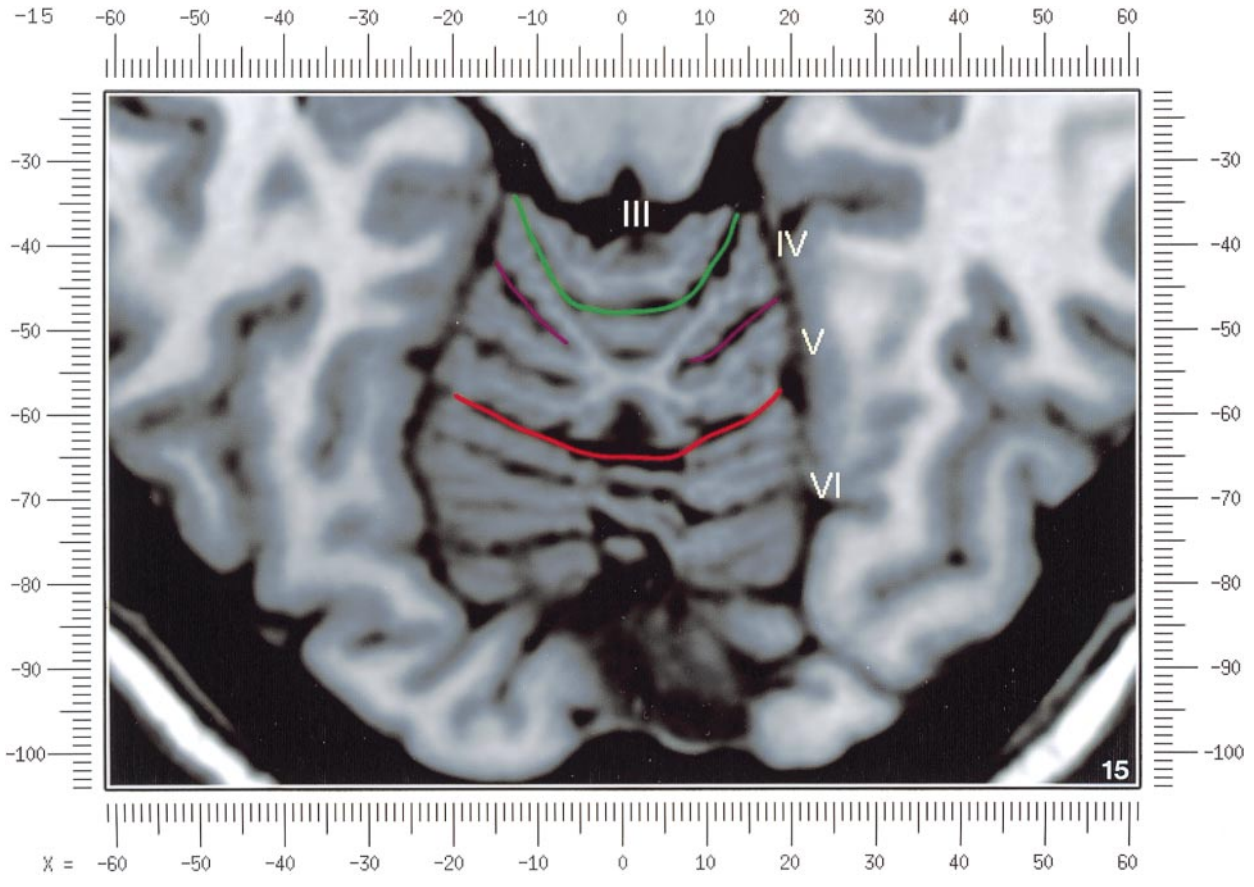

FIGURE 15

Nomenclature

The revised nomenclature proved to be simple and reliable. The names of the fissures were not changed, as they are anatomically consistent, have historic significance, and are still widely used and understood. In contrast, we dispensed with the Latin names of the lobules, and used Larsell's Roman numeral designations with some revisions. Table 1 presents the nomenclature used in this atlas to describe the cerebellar fissures and lobules. Table 2 presents a comparison of the earlier nomenclature systems with that derived from this atlas (based on Larsell). This table is helpful when drawing anatomic correlations between studies that employ different nomenclatures. The detailed discussion of the various nomenclatures through the years, and the way that this atlas, and particularly the use of the Display software, allowed for the resolution of the apparent conflicts is beyond the scope of this paper.

Views of the Cerebellum in the Sagittal, Coronal, and Horizontal Planes

Selected sections of the cerebellum are presented in the parasagittal (Figs. 4–14), horizontal (Figs. 15–20), and coronal planes (Figs. 21–27), showing the progression of the fissures and lobules from midline to lateral; superior to inferior; and anterior to posterior. The fissures are color coded, according to the table. Selected cryosections of postmortem brain show the locations and anatomic structures of the deep nuclei in the parasagittal (Figs. 5 (bottom), 6 (bottom), 10 (bottom), 11 (bottom)), horizontal (Fig. 17 (bottom)), and coronal planes (Figs. 21 (bottom), 22 (bottom)).

Three-Dimensional Images

The three-dimensional reconstruction of the fissures provides a new view of the fissures as they course through the cerebellum and subdivide it into lobules

FIGS. 15–19. Axial images of the cerebellum commencing at $z = -15$ and progressing inferiorly to $z = -55$.

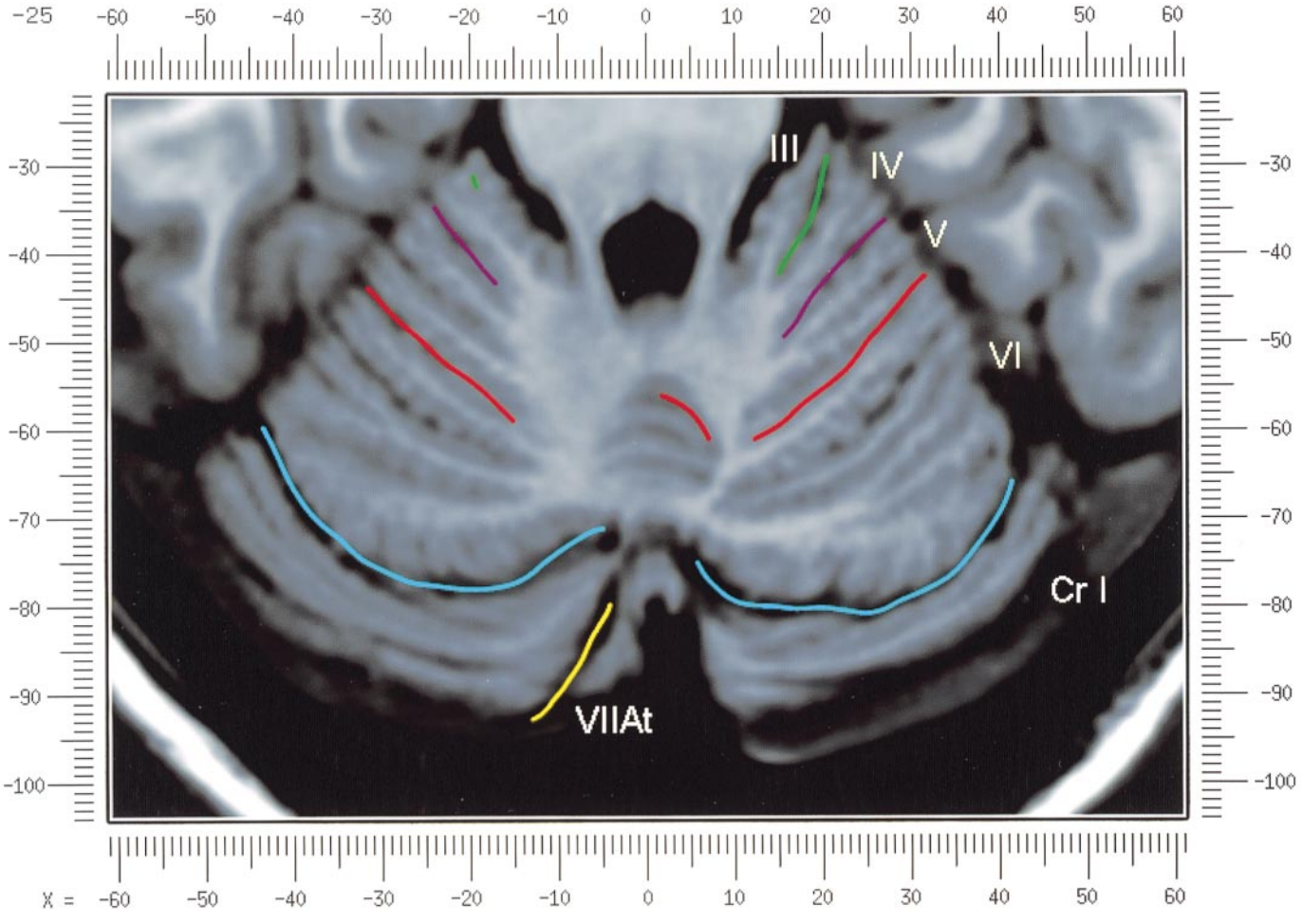

FIGURE 16

(Fig. 2). The 3-dimensional renditions of the superior and posterior surface views of the cerebellum (shown as stereo-pairs in Fig. 3) reveal the external location of the fissures and the parcellation of the cerebellar surface into lobules.

Description of the Fissures and Lobules

Vermal lobules I and II were indistinguishable and abut the anterior medullary velum, which lies anterior and inferior to the vermis. There is no hemispheric extension of vermal lobule I. Hemispheric lobule II is the lateral extension of I and II. Lobule I is distinct from lobule II in some human cerebella and in lower primates. This distinction is thus maintained, even though it is not always apparent. The vermal and hemispheric components of lobule I/II have together been termed the lingula.

The precentral fissure separates lobules I and II from lobule III (centralis), both in the vermis and the hemispheres. Lobule III is partially obscured by lobule IV when viewed from the superior aspect, but it is sizeable, has a semilunar form, and is the first distinct folium not attached to the superior medullary velum.

The preculminate fissure separates lobule III from lobule IV.

The use of the older term "culmen" (including both the vermis and the hemisphere) obscures the fact of the division of the culmen into lobules IV and V by the intraculminate fissure. This fissure is readily discernible on the hemisphere, but at the midline is continuous with a small fissure situated between the branches of a folium and thus can be difficult to localize with accuracy in the absence of adjacent sagittal sections or surface reconstructions. In this brain it was possible to trace the intraculminate fissure from the right hemisphere across the midline to the left side. By using the coronal images (see $y = -46$) we determined that the three major folia of the "culmen" are subdivided such that lobule IV contains one folium, and lobule V contains two.

The primary fissure distinguishes the anterior lobe of the cerebellum (lobules I through V) from the posterior

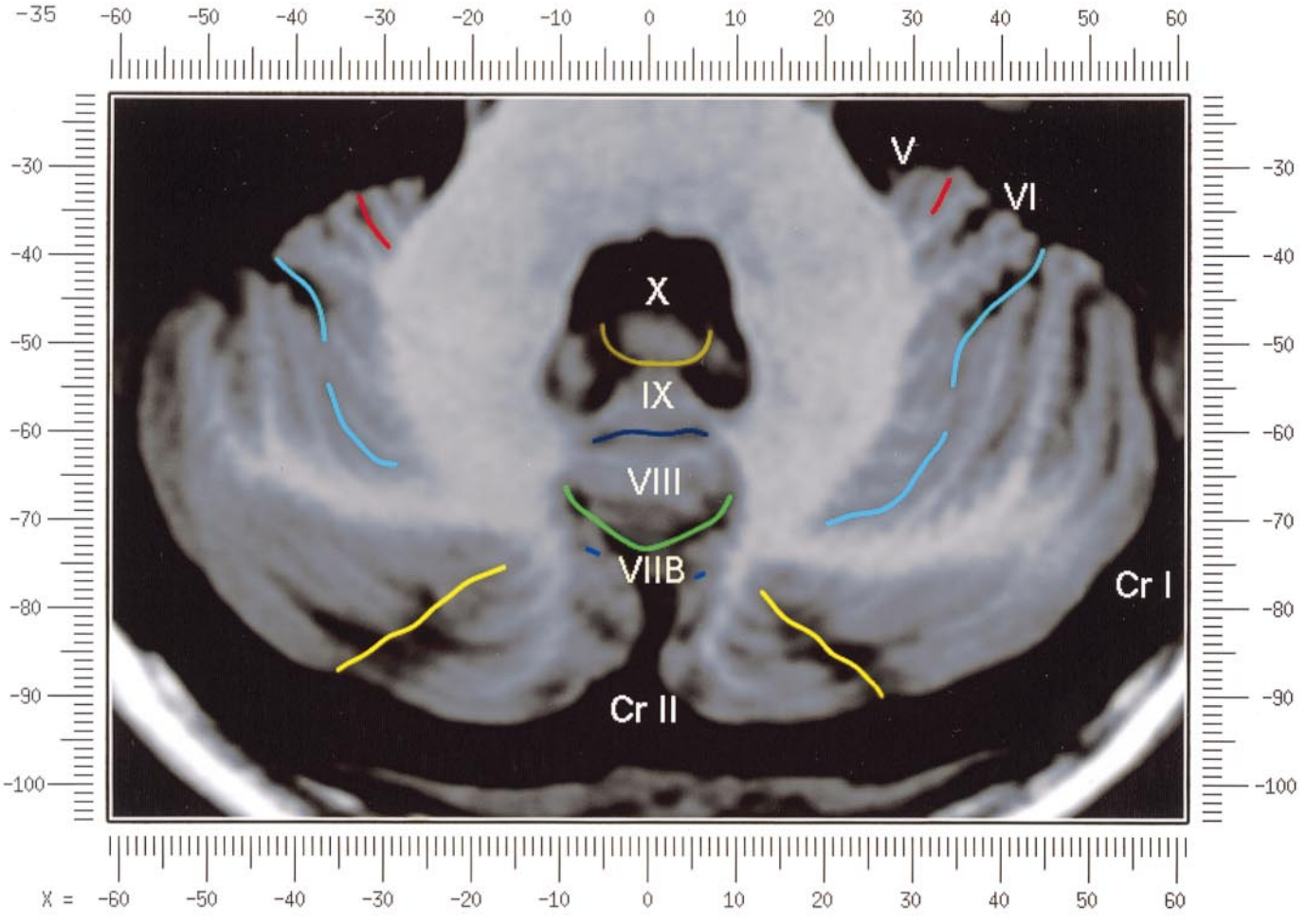

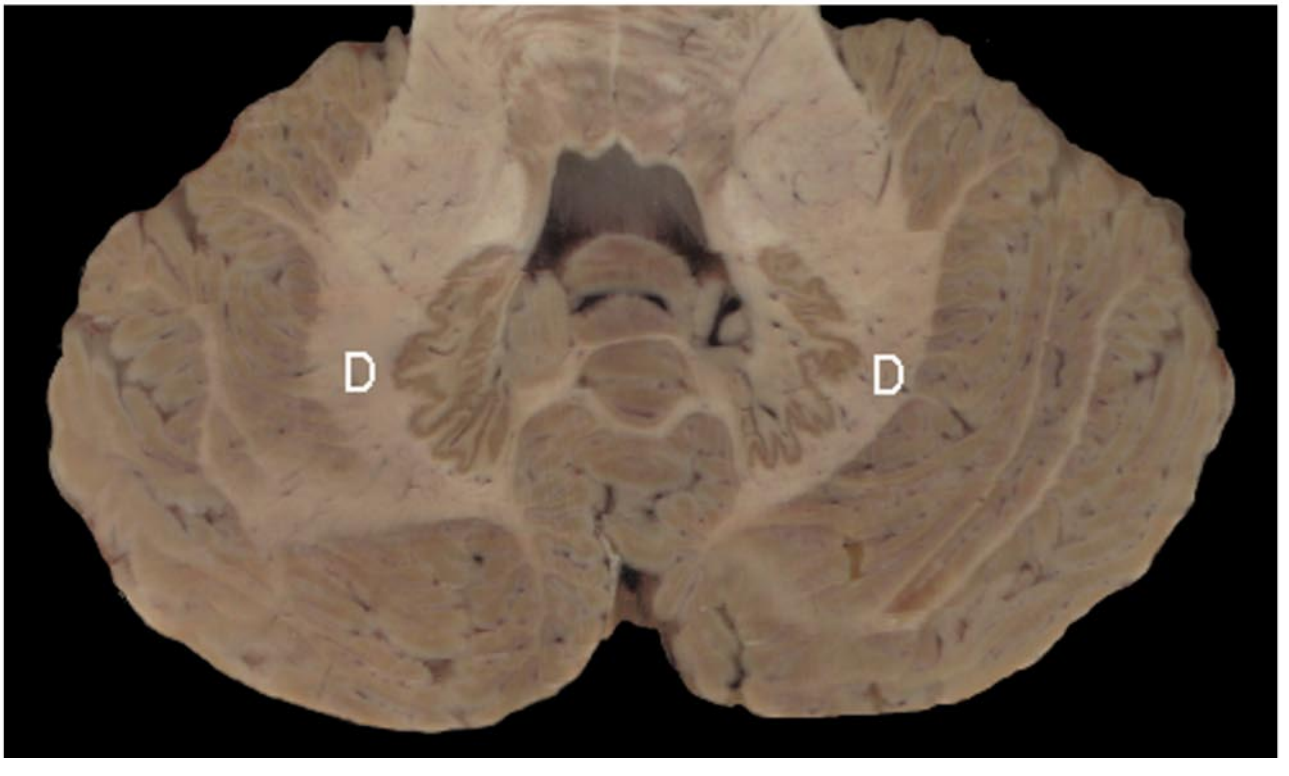

FIG. 17. A cryosection in the axial plane corresponding to $z = -35$. D, dentate nucleus.

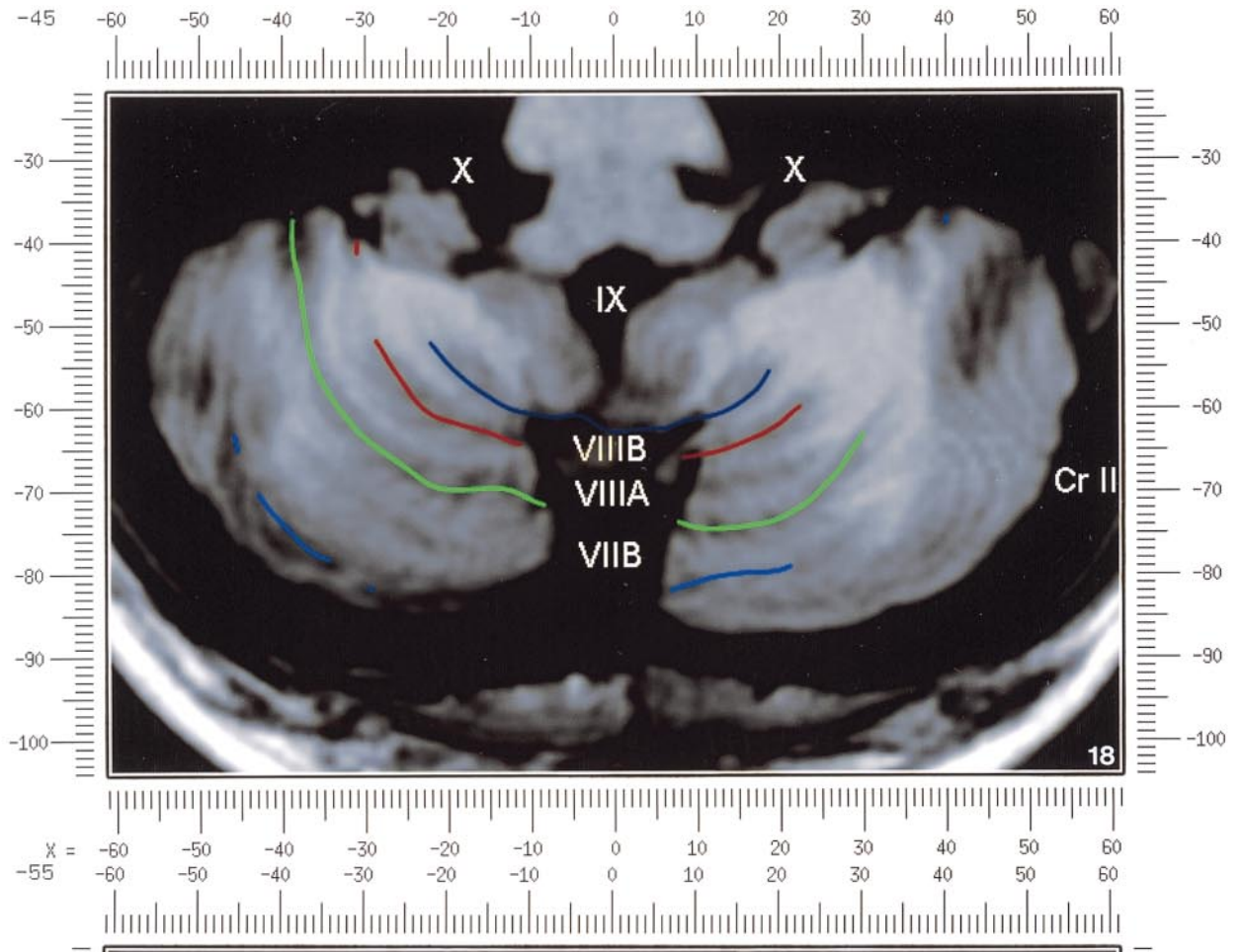

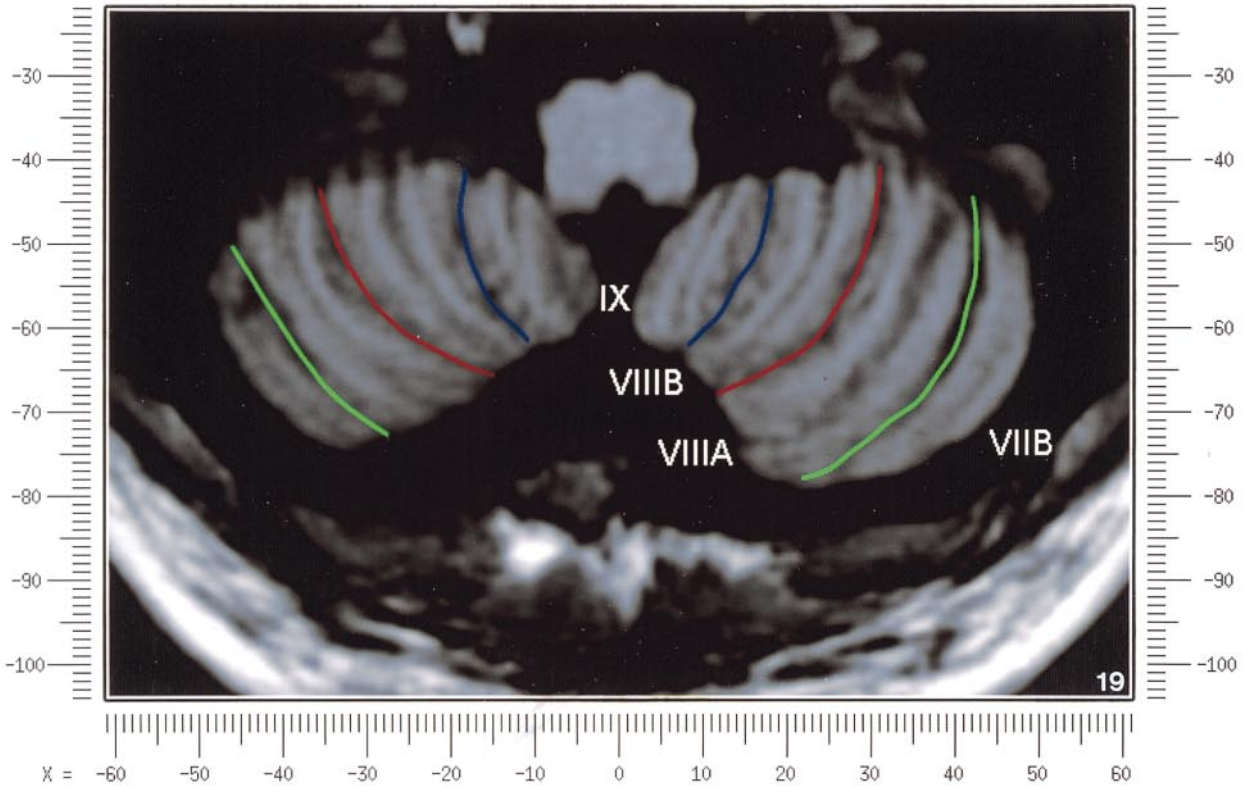

FIGURES 18 & 19

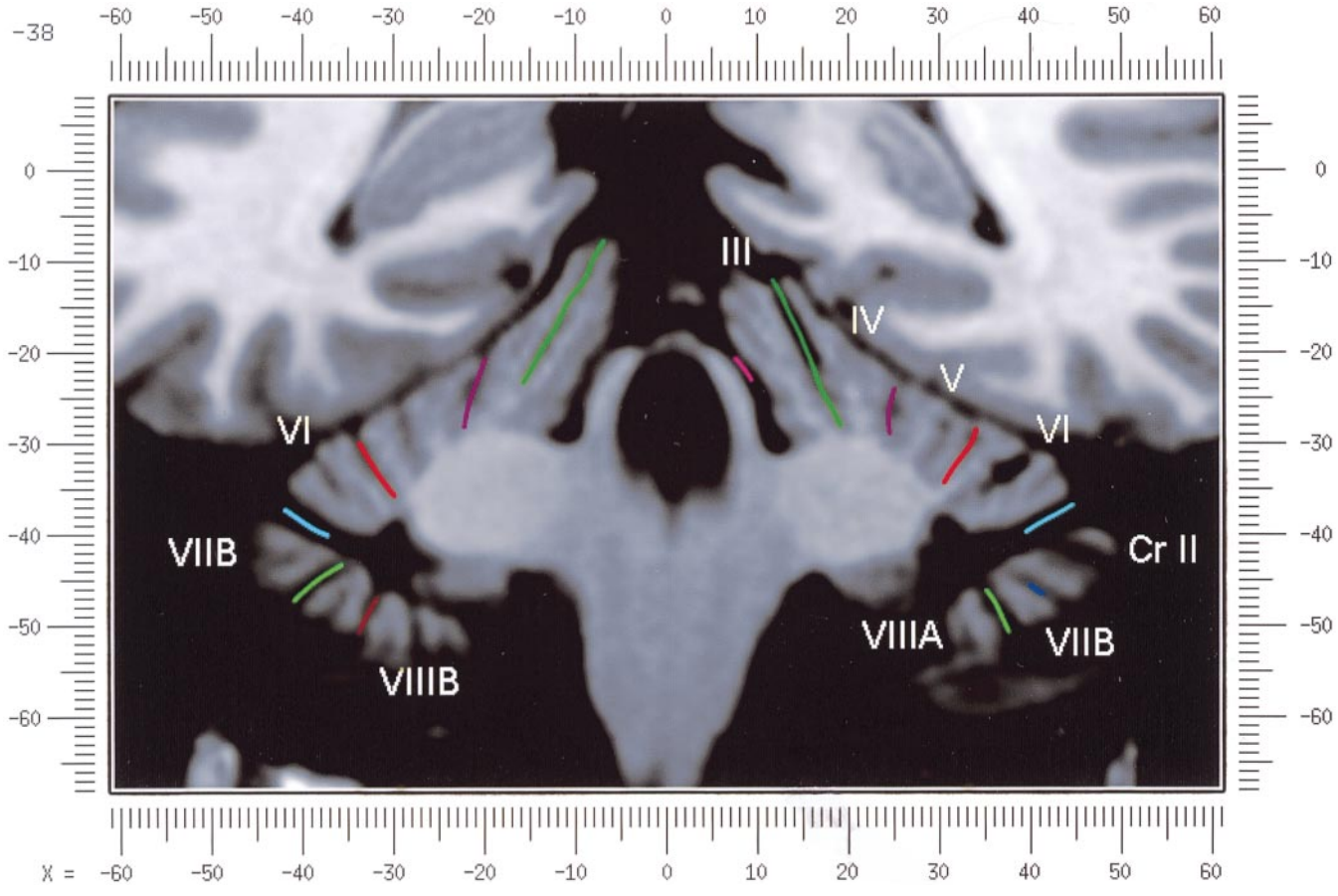

FIGS. 20–25. Coronal images of the cerebellum commencing at $y = -38$ and progressing caudally to $y = -88$.

lobe (lobules VI through IX), and specifically it separates lobule V from lobule VI, both in the vermis and the hemisphere. The primary fissure and other fissures within the anterior lobe are progressively more difficult to discern on parasagittal sections as one moves laterally away from the midline. The primary fissure is unmistakable on midsagittal section but it is continuous with an undistinguished small fissure in the intermediate sectors of the hemispheres.

The superior posterior fissure appears early in development and is visible in this brain on the 3-D reconstruction of the superior surface (Fig. 3). Lobule VI lies between the primary and superior posterior fissures and is therefore sizeable and contains two large folia with medullary rays that take their origin off the medullary core (e.g., see $y = -58$). The vermal and hemispheric components of lobule VI have previously received different names. Lobule VI in the vermis was called the declive, and in the hemisphere it has received the name lobulus simplex among others (see Table 2).

The superior posterior fissure separates lobule VI from lobule VII in the vermis and lobule VI from crus I (of the ansiform lobule) in the hemisphere.

Vermal lobule VII is complex and its lateral extension into the ansiform lobule of Bolk forms a large part of the hemisphere in the human cerebellum. The terms folium and tuber have been used to denote vermis VII, but this fails to convey the complexity of the equivalent hemispheric extensions. Further, VIIA (in the Larsell terminology) is divided by the horizontal fissure into two sectors, with important differences in their hemispheric extensions.

Vermal lobule VIIAf (identical to the folium) expands laterally to form crus I (of the ansiform lobule). Vermal lobule VIIAt (previously the rostral half of the tuber) corresponds in the hemisphere with crus II. The horizontal fissure separates VIIAf from VIIAt in the vermal region, and crus I from crus II in the hemispheres. In this brain, VIIAf is not present in the midline. It appears at 6 mm to the right of midline and 4 mm to the left of midline. For this reason, in the midsagittal plane and just lateral to it, the superior posterior fissure is bounded caudally by the ansoparamedian and not the horizontal fissure.

The ansoparamedian fissure is submerged on the ventral surface of the "tuber," separating lobules VIIAt from VIIB (previously termed the paramedian or gracile lobule). The precise delineation of this fissure and the division of crus II from VIIB in the hemisphere has long been the subject of controversy. We were able to

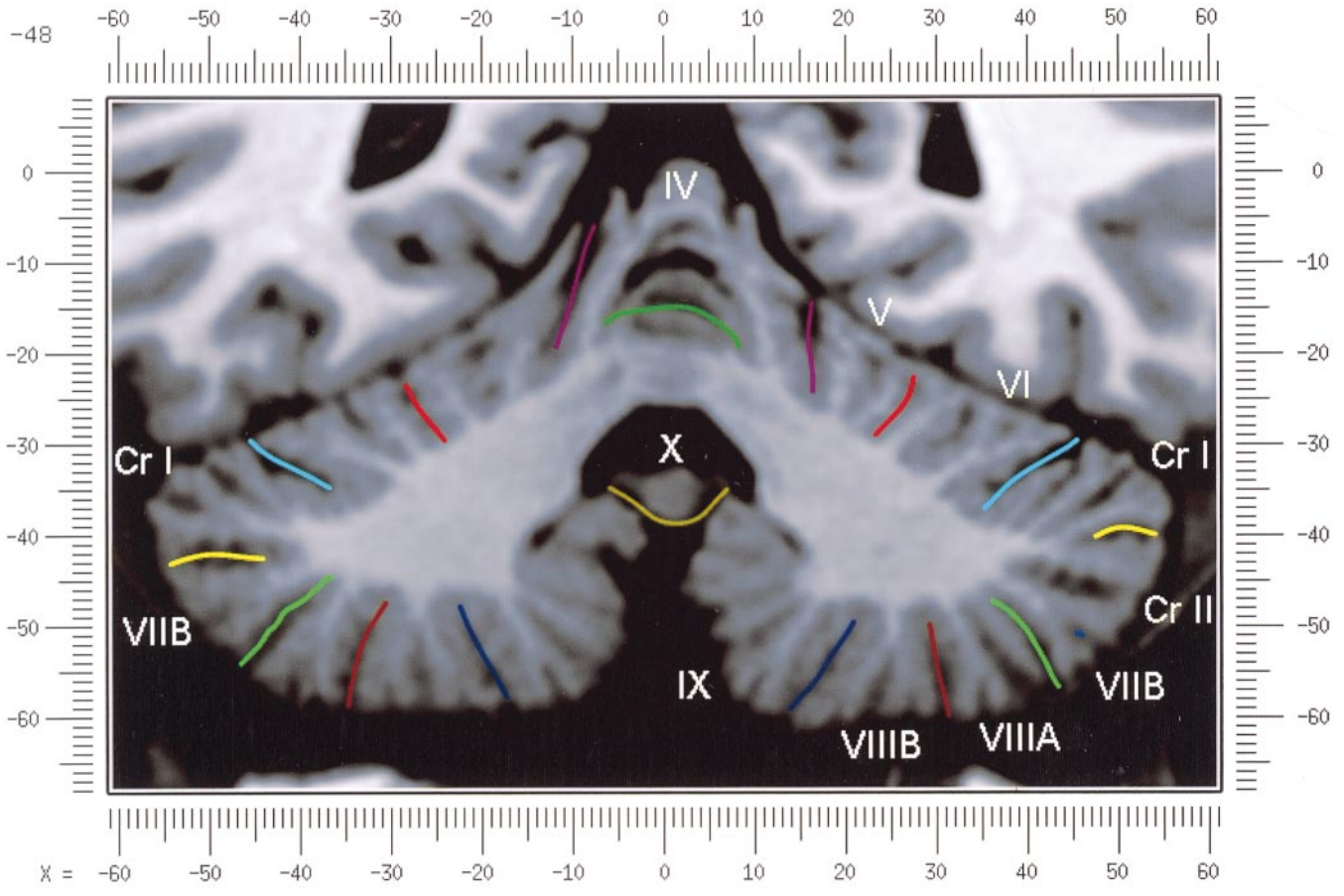

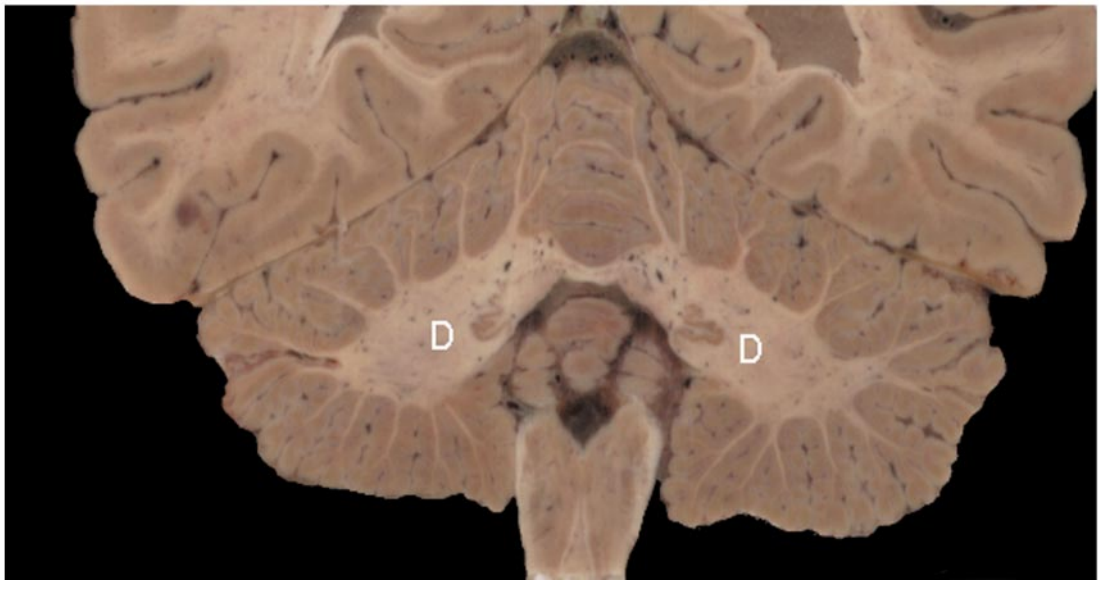

FIG. 21. Bottom: A cryosection in the coronal plane corresponding to $y = -48$. D, dentate nucleus.

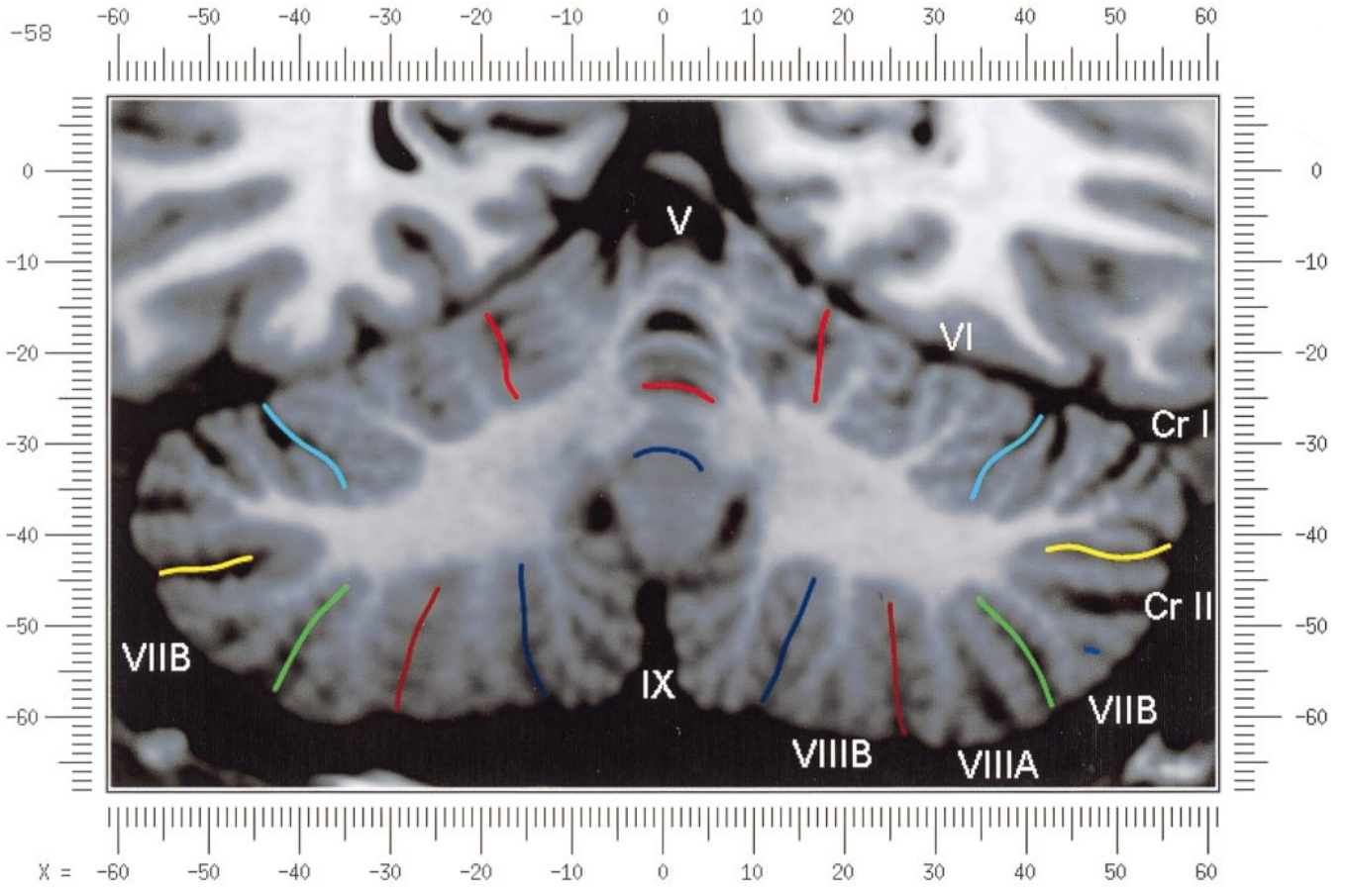

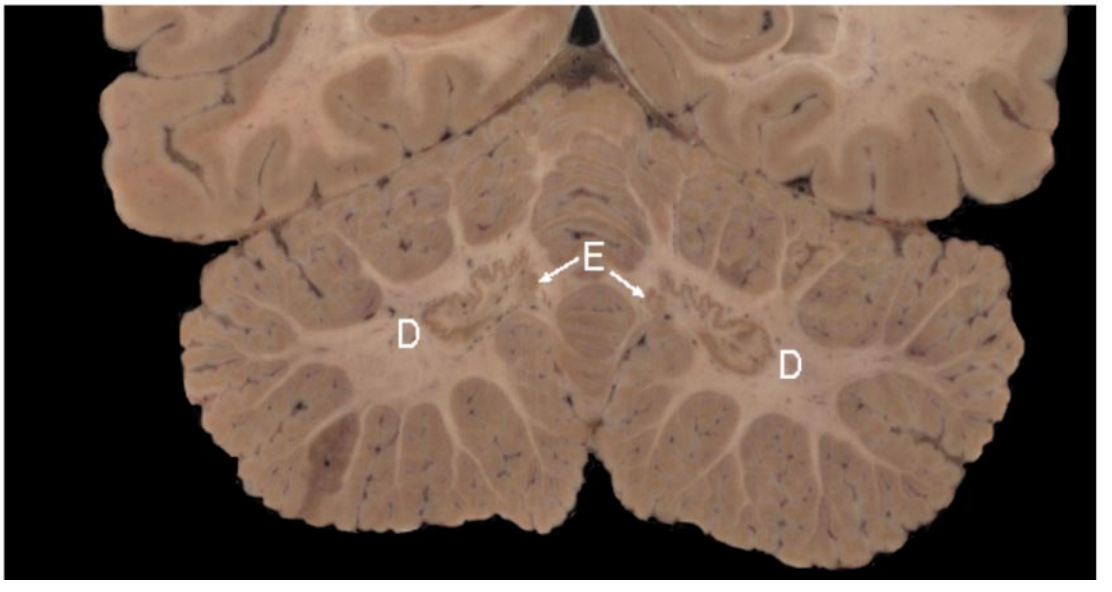

FIG. 22. Bottom: A cryosection in the coronal plane corresponding to $y = -58$. D, dentate nucleus; E, emboliform nucleus.

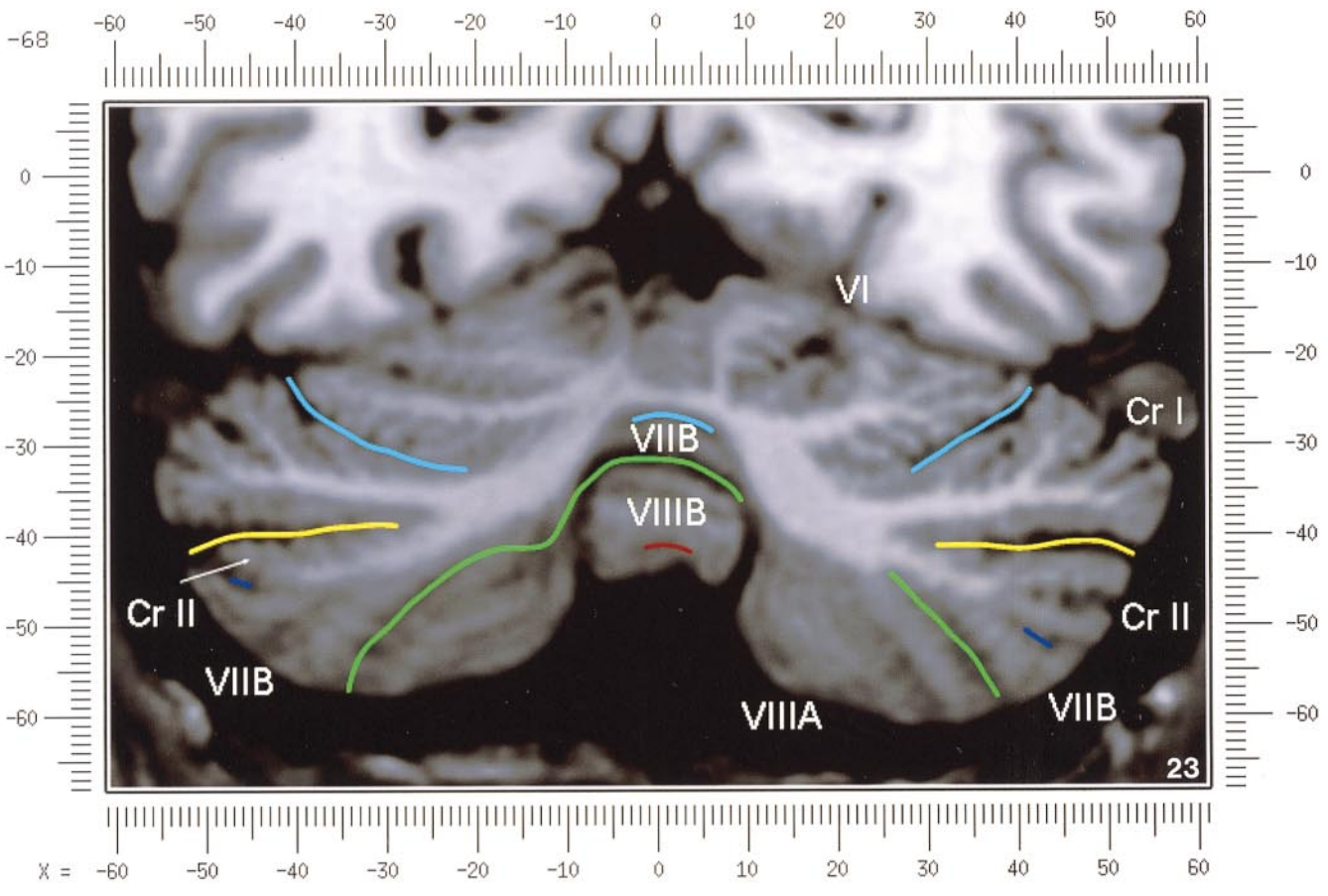

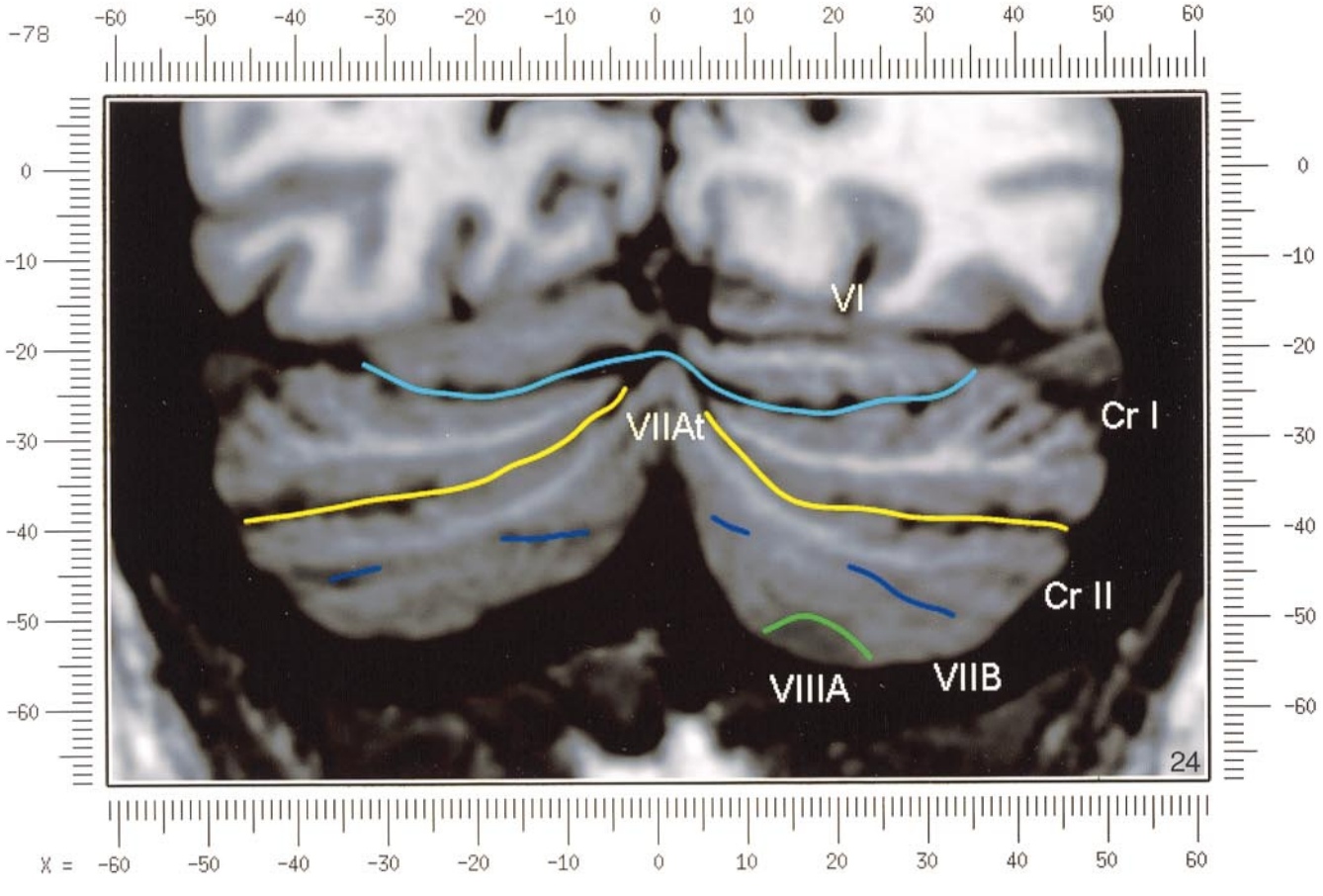

FIGURES 23 & 24

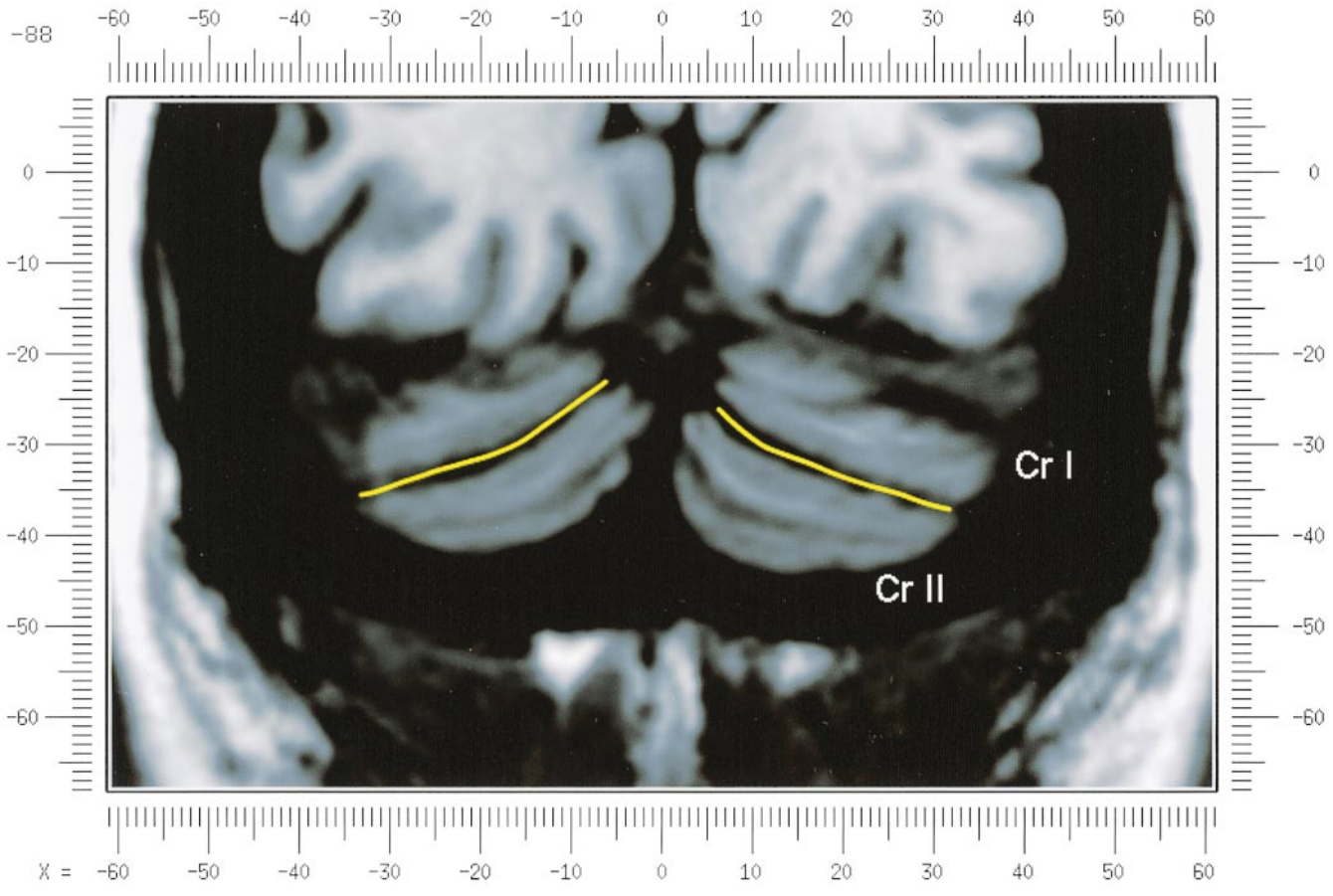

FIGURE 25

delineate this fissure, but in following the ansoparamedian fissure from the midline laterally, an asymmetry was revealed in the delineation of crus II. This occurred because on the left side the horizontal and ansoparamedian fissures meet on the posterior inferior cerebellar surface. Crus II on the left therefore is a triangular lobe situated on the superior and the posterior aspects of the posterior lobe. On the right side, however, the horizontal and ansoparamedian fissures do not meet, thus revealing that crus II continues laterally and forward onto the anterior surface of the cerebellum. The effect of this asymmetry is that on lateral sagittal sections, crus I is adjacent to lobule VIIB on the left, whereas on the right crus II is adjacent to VIIB. This asymmetry may help explain some of the earlier debate as to whether VIIB is distinct from the inferior semilunar lobule (see, e.g., Basle Nomina Anatomica, 1895; Smith, 1902; Ziehen, 1934; Larsell and Jansen, 1972). Coronal sections in this brain (see $y = -54$ through -74) confirm that despite the fact that the folia at the lateral inferior cerebellar surface are asymmetric across the two hemispheres, they are derived from medullary rays that are morphologically similar.

The prepyramidal/prebiventer fissure separates VIIB from VIIIA. It is named according to whether the VIIB/VIIIA distinction is in the vermis (prepyramidal fissure) or hemisphere (prebiventer fissure). The intrabiventer fissure separates VIIIA from VIIIB. (The term "intrapyramidal" was omitted for purposes of simplification.)

The secondary fissure is interposed both at the vermis and in the hemispheres between VIIIB and IX (in the older terminology—uvula at the vermis; tonsil or ventral and accessory paraflocculus at the hemisphere).

The posterolateral fissure forms the boundary between the posterior lobe of the cerebellum and the flocculonodular lobe, separating IX from X (in the older terminology—nodulus at the vermis; flocculus at the hemisphere).

DISCUSSION

The understanding of the human cerebellum has been substantially advanced by the availability of detailed anatomic images revealed by conventional MRI and by cerebellar activation with PET and fMRI studies of motor, sensory, and cognitive/emotional functions (see, e.g., Desmond *et al.*, 1998; Doyon, 1997; Elliott and Dolan, 1998; Fiez and Raichle, 1997; Parsons and Fox, 1997). Until now, determining the precise

location of lesions or sites of activation within the cerebellum has been limited by the lack of a sufficiently detailed and practical atlas. The MRI atlas that we have developed addresses this need.

This atlas has relied upon high-resolution anatomic images and Display software that permits simultaneous visualization of a cursor in the three cardinal planes within the cerebellum and 3-D reconstruction of the data. The resulting atlas of a human cerebellum extends the understanding of the gross morphology and organization of the cerebellum to a previously impenetrable level. It clarifies the anatomy of the human cerebellum, provides correlations of vermal with hemispheric structures, and defines the cerebellar lobules and folia. It demonstrates the details of the cerebellar cortex within the three cardinal planes in Talairach proportional stereotaxic space and makes this material available and useful to clinicians and investigators interested in the study of the cerebellum. An immediate consequence of this new understanding of cerebellar anatomy is a revised and more contemporary and accessible cerebellar nomenclature.

It is hoped that this atlas will facilitate the study of a number of anatomical–functional–pathological questions that could not previously be addressed. The possibility of predictable cerebellar hemispheric asymmetries and the constancy of the location and pattern of the cerebellar fissures and lobules may now be studied by comparing identifiable cerebellar landmarks between different individuals. This atlas may serve as the basis for future morphometric analyses and probabilistic maps of the human cerebellum and permit quantitative estimations and comparisons to be made regarding the size of different lobules and folia. Morphometric analysis will be necessary to determine the changes, if any, that occur with normal aging and in cerebellar diseases and for accurately monitoring rate and degree of atrophy once treatment options become available for degenerative diseases of the cerebellum. We have recently used this atlas to develop a semiflattened map onto which we charted the results of a meta-analysis of published functional imaging studies, suggesting that there are distinct motor and cognitive maps in the cerebellum (Schmahmann *et al.*, 1998).

The imprecise definition of the deep cerebellar nuclei by even this high resolution MRI technique was somewhat disappointing and is most likely a reflection of their anatomic organization. The dentate nucleus is composed of a relatively thin and convoluted layer of neurons; the fastigial nucleus is a flattened plate of neurons adjacent to the midline; and the globose and emboliform nuclei interposed between them have rather indistinct borders. This methodological limitation of the current MRI technology was partially compensated for by comparing the MRI sections with digitized images warped into Talairach space of postmortem cryosections of another brain (Toga *et al.*, 1997). The use of these two complimentary techniques provided necessary additional detail of the cerebellar nuclear anatomy.

In summary, we have used high resolution MR images and software that permits simultaneous cross-correlation in the three cardinal planes to develop a detailed atlas of a human cerebellum in stereotaxic proportional space including three-dimensional representations of the external surface and fissures. This approach substantially advances our understanding of the anatomy of the human cerebellum and should prove valuable in future studies of its organization and function.

ACKNOWLEDGMENTS

This work was supported in part by the National Library of Medicine (J.D.S.). Nikos Makris, Ph.D., and David Kennedy, Ph.D., provided valuable input in the early stages of this project. The assistance of librarians in the Rare Book Collections of the New York Academy of Medicine and in the Countway Library of Medicine at Harvard Medical School is appreciated. The assistance of Marygrace Neal M.Ed. in the preparation of this manuscript is gratefully acknowledged. Presented in part at the 2nd International Conference on Functional Mapping of the Human Brain, June 1996, Boston, MA.

REFERENCES

Anatomical Society of Great Britain and Ireland. 1933. Final report of the committee appointed by the Anatomical Society of Great Britain and Ireland on June 22, 1928. Robert Maclehose and Co., Ltd., University Press, Glasgow. (Birmingham Revision of the Basle Nomina Anatomica; BNA-BR.).

Angevine, J. B., Mancall, E. L., and Yakovlev, P. I. 1961. *The Human Cerebellum: An Atlas of Gross Topography in Serial Sections.* Little, Brown and Co., Boston.

Ariëns Kappers, C. U., Huber, G. C., and Crosby, E. C. 1936. *Comparative Anatomy of the Nervous System of Vertebrates, Including Man*, Vol. 1. Macmillan, New York.

Bowden, D. M., and Martin, R. F. 1995. Neuronames brain hierarchy. *Neuroimage* **2:**63–83.

Bradley, O. C. 1904. The mammalian cerebellum: Its lobes and fissures, part 1. *J. Anat. Physiol.* **38:**448–475.

Bolk, L. 1906. *Das Cerebellum der Saeugetiere.* Bohn and Fischer, Jena.

Carpenter, M. B. 1976. *Human Neuroanatomy.* Williams & Wilkins, Baltimore, MD.

Collins, D. L., Neelin, P., Peters, T. M., and Evans, A. C. 1994. Automatic 3D intersubject registration of MR volumetric data in standardized Talairach space. *J. Comput. Assist. Tomogr.* **18:**192–205.

Courchesne, E., Press, G. A., Murakami, J., Berthoty, D., Grafe, M., Wiley, C. A., and Hesselink, J. R. 1989. The cerebellum in sagittal plane—Anatomic–MR correlation: 1. The Vermis. *Am. J. Nerol. Res.* **10:**659–665.

Crosby, E. C., Humphrey, T., and Lauer, E. W. 1962. *Correlative Anatomy of the Nervous System*, pp. 188–192. Macmillan, New York.

DeArmond, S. J., Fusco, M. M., and Devey, M. M. 1976. *A Photographic Atlas: Structure of the Human Brain.* Oxford Univ. Press, New York.

Dejerine, J. 1901. *Anatomie des Centres Nerveux*, Tome 2. J. Rueff et Cie, Paris.

Desmond, J. E., Gabrieli, J. D., and Glover, G. H. 1998. Dissociation of frontal and cerebellar activity in a cognitive task: Evidence for a distinction between selection and search. *Neuroimage* **7:**368–376.

Dow, R. S. 1942. The evolution and anatomy of the cerebellum. *Biol. Rev.* **17:**179–220.

Doyon, J. 1997. Skill learning. In *The Cerebellum and Cognition*. (J. D. Schmahmann, Ed.) *Int. Rev. Neurobiol.* **41:**273–296. Academic Press, San Diego.

Edinger, L. 1909. Uber die Enteilung des Cerebellums. *Anatomischer. Anzeiger* **35:**319–323.

Elliott, R., and Dolan, R. J. 1998. Activation of different anterior cingulate foci in association with hypothesis testing and response selection. *Neuroimage* **8:**17–29.

Fiez, J. A., and Raichle, M. E. 1997. Linguistic processing. In *The Cerebellum and Cognition* (J. D. Schmahmann, Ed.) *Int. Rev. Neurobiol.* **41:**233–254. Academic Press, San Diego.

Flatau, E., and Jacobsohn, L. 1899. *Handbuch der Anatomie und vergleichende Anatomie des Centralnervensystems der Saeugetiere. I. Makroskopischer Teil.* Karger, Berlin.

Henle, J. 1901. *Grundriss der Anatomie des Menschen, Neu bearbeitet von F. Merkel,* 4th Aufl. Atlas. Friedrich Vieweg & Sohn, Braunschweig.

His, W. 1895. *Die anatomische Nomenklatur. Nomina anatomica. Separat-Abzug aus Archiv für Anatomie und Physiologie. Anatomische Abteilung,* Supplement-Band (Basle Nomina Anatomica of 1895).

Holmes, C. J., Hoge, R., Collins, L., Woods, R., Toga, A. W., and Evans, A. C. 1998. Enhancement of MR images using registration for signal averaging. *J. Comput. Assist. Tomogr.* **22:**324–33.

Ingvar, S. 1918. Zur Phylo- und Ontogenesae des Kleinhirns. *Folia Neuro-Biologica* **11:**205–495.

Ingvar, S. 1928. The phylogenetic continuity of the central nervous system. In *Studies in Neurology,* Vol. I. *Bull. Johns Hopkins Hosp.* **43:**315–337.

International Anatomical Nomenclature Committee. 1956. *Nomina Anatomica.* Revised by the I.A.N.C. appointed by the Fifth International Congress of Anatomists held at Oxford in 1950. Submitted to the Sixth International Congress of Anatomists, held in Paris, July 1955. Williams & Wilkins, Baltimore.

Jakob, A. Das Kleinhirn. 1928. In (*v. Möllendorff's*) *Handbuch der mikroskopischen Antomie des Menschen,* Vol. 4, pp. 674–916. Springer, Berlin.

Jansen, J., and Brodal, A. 1958. Das Kleinhirn. In (*v. Möllendorff's*) *Handbuch der mikroskopischen Antomie des Menschen,* Vol. 4, pp. 1–323. Springer, Berlin.

Kretschmann, H. J., and Weinrich, W. 1992. Cranial neuroimaging and clinical neuroanatomy. Thieme, New York.

Kuithan, W. 1894. Die Entwicklung des Kleinhirns von Säugetieren, unter Ausschluß der Histogenese. *Sitzungsbericht der Gesellschaft für Morphologie und Physiologie, München* **10:**89–128.

Langelaan, J. W. 1919. On the development of the external form of the human cerebellum. *Brain* **42:**130–170.

Larsell, O. 1934. Morphogenesis and evolution of the cerebellum. *Arch. Neurol. Psychiatry* **31:**373–395.

Larsell, O. 1937. The cerebellum: A review and interpretation. *Arch. Neurol. Psychiatry* **38:**580–607.

Larsell, O. 1947. The development of the cerebellum in man in relation to its comparative anatomy. *J. Comp. Neurol.* **87:**85–129.

Larsell, O. 1953. The anterior lobe of the mammalian and the human cerebellum. *Anat. Rec.* **115:**341.

Larsell, O. 1958. Lobules of the mammalian and human cerebellum. *Anat. Rec.* **130:**329–330.

Larsell, O. 1967. *The Comparative Anatomy and Histology of the Cerebellum from Myxinoids through Birds.* (J. Jansen, Ed.) Univ. Minnesota Press, Minneapolis.

Larsell, O. 1970. *The Comparative Anatomy and Histology of the Cerebellum from Monotremes through Apes.* (J. Jansen, Ed.) Univ. Minnesota Press, Minneapolis.

Larsell, O., and Jansen, J. 1972. *The Comparative Anatomy and Histology of the Cerebellum. The Human Cerebellum, Cerebellar Connections, and Cerebellar Cortex.* Univ. Minnesota Press, Minneapolis.

Lorenson, W. E., and Cline, H. E. 1987. Marching cubes: A high resolution surface reconstruction algorithm. *Comput. Graphics* **4:**163–169.

Loyning, Y., and Jansen, J. 1955. A note on the morphology of the human cerebellum. *Acta Anatomica* **25:**309–318.

Madigan, J. C., and Carpenter, M. B. 1971. *Cerebellum of the Rhesus Monkey: Atlas of Lobules, Laminae, and Folia, in Sections.* University Park Press, Baltimore.

Malacarne, M. V. G. 1776. *Nuova esposizione della vera struttura del cerveletto umano.* Briolo, Torino.

Meckel, J. F. 1838. *Manual of Descriptive and Pathological Anatomy.* Volume II (Translated from German into French by A. J. L. Jourdan and G. Breschet. Translated from French into English by A. S. Doane.) E. Henderson, Old Bailey, London.

Parsons, L. M., and Fox, P. T. 1997. Sensory and cognitive functions. In *The Cerebellum and Cognition* (J. D. Schmahmann, Ed.) *Int. Rev. Neurobiol.* **41:**255–272. Academic Press, San Diego.

Press, G. A., Murakami, J., Courchesne, E., Berthoty, D., Grafe, M., Wiley, C. A., and Hesselink, J. R. 1989. The cerebellum in sagittal plane—Anatomic–MR correlation: 2. The cerebellar hemispheres. *Am. J. Neurol. Res.* **10:**667–676.

Press, G. A., Murakami, J., Courchesne, E., Grafe, M., and Hesselink, J. R. 1990. The cerebellum: 3. Anatomic–MR correlation in the coronal plane. *Am. J. Neurol. Res.* **11:**41–50.

Riley, H. A. 1929. The mammalian cerebellum. A comparative study of the arbor vitae and folial pattern. *Res. Publ. Assoc. Res. Nervous Mental Dis.* **6:**37–192.

Riley, H. A. 1930. The lobules of the mammalian cerebellum and cerebellar nomenclature. *Arch. Neurol. Psychiatry* **24:**227–256.

Roberts, M. P., Hanaway, J., and Morest, D. K. 1987. *Atlas of the Human Brain in Sections.* Lea & Febiger, Philadelphia.

Schäfer, E. A., and Symington, J. Neurology. 1908. In *Quain's Elements of Anatomy,* 11th ed., pp. 167–201. Longmans, Green & Co, London.

Schmahmann, J. D., Hurwitz, A. S., Loeber, R. T., and Marjani, J. L. 1998. A semi-flattened map of the human cerebellum. A new approach to visualizing the cerebellar cortex in 2-dimensional space. *Soc. Neurosci. Abstr.* **24:**1409.

Schmahmann, J. D., Loeber, R. T., Marjani, J., and Hurwitz, A. S. 1998. Topographic organization of cognitive functions in the human cerebellum. A meta-analysis of functional imaging studies. *NeuroImage* **7:**S721.

Schwalbe, G. A. 1881. *Lehrbuch der Neurologie.* Eduard Besold, Erlangen.

Smith, G. E. 1902. The primary subdivision of the mammalian cerebellum. *J. Anat. Physiol.* **36:**381–385.

Stroud, B. B. 1895. The mammalian cerebellum. *J. Comp. Neurol.* **5:**71–118.

Talairach, J., Tournoux, P. 1988. *Co-Planar Stereotaxic Atlas of the Human Brain. 3-Dimensional Proportional System: An Approach to Cerebral Imaging* (Translated by Mark Rayport.) Thieme, New York.

Toga, A. W., Goldkorn, A., Ambach, K., Chao, K., Quinn, B. C., and Yao, P. 1997. Postmortem cryosectioning as an anatomic reference for human brain mapping. *Comput. Med. Imaging Graph.* **21:**131–41.

Vicq-d'Azyr, F. 1786. *Traité d' anatomie et de physiologie, avec des planches coloriées,* Tome premier. Francois Ambrose Didot l'aîné, Paris.

Waddington, M. M. 1984. *Atlas of Human Intracranial Anatomy.* Academic Books, Rutland, VT.

Ziehen, T. 1934. *Centralnervensystem. Handbuch der Anatomie,* pp. 1230–1289. Verlag von Gustav Fischer, Jena.